physica status solidi

pss

www.interscience.wiley.com

reprints

www.pss-rrl.com

www.pss-c.com

www.pss-b.com

www.pss-a.com

WILEY-VCH

REPRINT

Phys. Status Solidi B **246**, No. 1, 9–31 (2009) / **DOI** 10.1002/pssb.200844238

physica status solidi b
www.pss-b.com
basic solid state physics

Feature Article

Pressure-induced structural phase transitions in materials and earth sciences

Francisco Javier Manjón[*,1] **and Daniel Errandonea**[2]

[1] MALTA Consolider Team, Departamento de Física Aplicada-IDF, Universitat Politècnica de València, Cno. de Vera s/n, 46022 València, Spain
[2] MALTA Consolider Team, Departamento de Física Aplicada-ICMUV, Fundación General de la Universitat de València, Edificio de Investigación, c/Dr. Moliner 50, 46100 Burjassot (València), Spain

Received 7 June 2008, revised 6 October 2008, accepted 16 October 2008
Published online 28 November 2008

PACS 07.35.+k, 61.50.Ks, 62.50.Ef, 64.70.K–

[*] Corresponding author: e-mail fjmanjon@fis.upv.es, Phone: +34 963 877 000, Fax: +34 963 877 09

Pressure is an important thermodynamic parameter since it allows an increase of matter density by reducing volume. The reduction of volume by applying high pressures leads to an overall decrease of interatomic and intermolecular distances that allows exploring in detail atomic and molecular interactions. Therefore, high-pressure research has improved our fundamental understanding of these interactions in solids, liquids and gasses. The study of the structure of matter under compression is a rapid developing field that is receiving increasing attention especially due to continuous experimental and theoretical developments. In this article, we give a brief description of the experimental and theoretical methods employed in the study of solid matter at high pressures and summarize the high-pressure phases of the most relevant elements and inorganic compounds of the AX, A_2X, AX_2, ABX_2, A_2X_3, ABX_3, ABX_4 and AB_2X_4 families giving an overview of the state of the art in high-pressure research by highlighting recent discoveries, hot spots, controversial questions, and future directions of research.

1 Introduction Pressure is an important thermodynamic parameter similar in importance to temperature. In fact, physical, chemical, and biological systems can be squeezed to reduce their overall interatomic and intermolecular distances over a much wider range than varying temperature. Consequently, the science of matter at high density is now changing our fundamental understanding of atomic and molecular interactions both in organic and inorganic matter and providing new insights into the properties of materials at ambient conditions. In fact, high-pressure science exceeds the domain of "hard" physical sciences to have a large impact on biology, ranging from commercial treatment of foodstuffs to investigating the origins of life. The study of the structure of matter at high pressures is a rapid developing field that is receiving increasing attention especially due to the use of the diamond-anvil cell (DAC) [1], the advent of modern third generation synchrotron facilities [2], well suited to the use of the DAC, and the theoretical advances in quantum mechanical computations [3, 4]. Additionally, experimental advances in laser-heating technology [5] have paved the way to the study of matter at high pressures and high temperatures like those present in the interior of planets.

During 2008 we celebrate the international year of the Planet Earth whose aim is to ensure greater and more effective use by society of the knowledge accumulated by the world's 400,000 Earth scientists. In this endeavor, high-pressure science is of primary importance since most of the matter at the solar system is subjected at pressures higher than 10 GPa and only a small fraction of matter at the surface of certain planets is exposed to what we call "ambient pressure" (0.1 MPa). Consequently, the knowledge of the structure of matter at high pressures is important to understand the behavior of the planetary and stellar interiors. Furthermore, the importance of knowing the structures of matter under compression is both of technological

and fundamental interest. For instance, high-pressure experiments on superconductors are being conducted to try to understand the mysteries of low- and high-temperature superconductivity by pressure-tunning their electrical and magnetical properties, and in solid-state chemistry the great challenge, as yet unmet, is to understand the fundamental principles governing the formation of crystal structures and to predict them for given conditions of temperature, pressure and composition. In the search for those fundamental principles the knowledge of the structure of matter at extreme conditions of pressures and temperatures is of inestimable help to test recent advances in quantum mechanical computations [6–10].

Francisco Javier Manjón received his Ph.D. in Physics from the University of Valencia in 1999. He did postdoctoral research at the Max Planck Institute for Solid State Research in Stuttgart (Germany) under a Marie Curie Fellowship of the European Union and, from 2001, is Professor of Physics at the Technical University of Valencia in Spain. Since 2007 he has been the principal scientist of the high pressure group at the Instituto para el Diseño y la Fabricación Automatizada (IDF). His research interests include the experimental and theoretical study of structural, electronic, and vibrational properties of semiconductors and insulators both at normal and extreme conditions of temperature and pressure with special emphasis on materials for solar cells and other optoelectronic applications. He is presently a member of the MALTA Consolider Consortium.

Daniel Errandonea is a Professor of Physics at the University of Valencia. His research explores the properties of materials over a broad range of thermodynamic conditions from low to very high pressures. He began his research career studying the effects of pressure in optical and electronic properties of semiconductors. An interest in geophysical subjects led him subsequently to the Max-Planck Institut für Chemie at Mainz (Germany) and the Geophysical Laboratory of the Carnegie Institution of Washington. There he extended his research to sophisticate techniques like the laser-heating of diamond-anvil cells. Since then, his research program has expanded to include high-pressure experimental and theoretical studies in condensed matter physics, earth and planetary science, and materials science. Some of his accomplishments include the measurement of the melting curves of different metals up to megabar pressures, the determination of the high-pressure structural sequence of different ternary compounds, and the discovery of pressure-induced phase transitions in rare-gas solids. He is also involved in the continued development of high-pressure techniques, including optical methods, synchrotron radiation techniques, and transport measurements. He is a fellow of the Alexander von Humboldt Foundation and won the Alvin Van Valkenburg Award among others. He is presently a member of the MALTA Consolider Consortium.

One of the major interests in high-pressure science is to synthesize materials with new or exotic properties that are not present in materials crystallized at ambient conditions but that can be found at the interior of the planets and stars and in both natural and man-made explosions. Since the properties of a material basically depend on the composition and crystal structure (also known as phase), to obtain materials with new properties by means of high pressure basically means: (i) to enclose a material with a certain composition in a container; and (ii) to apply pressure to the container in order to obtain a material with the same composition but displaying a different crystal structure or phase than that usually found at ambient conditions. When a material exposed to high pressures changes its crystal structure and symmetry it is said that it has suffered a pressure-induced structural phase transition. In many cases, the high-pressure phase can be recovered after pressure release, opening this way the door to the existence of metastable phases at ambient conditions. The most remarkable example is constituted by diamond, an allotropic phase of carbon metastable at ambient conditions which is the hardest material known to date. Diamond is a phase of tetrahedrally coordinated carbon obtained from hexagonal graphite at high pressures and temperatures which has recently been synthesized in nanocrystalline and microcrystalline forms near ambient pressure conditions [11]. The fact that artificial diamond growth was one of the first motivations to develop high pressure science evidences the interest in obtaining new hard materials synthesized at high pressures [12]. Nowadays, new ultrahard materials are being synthesized, like noble metal nitride PtN [13] which seems to be PtN_2 indeed**,** as discussed in Ref. [14], and several materials of M_3N_4 (M = C, Si, Ge, Sn, Ti, Zr, Hf) composition [14]. In fact, it has to be confirmed experimentally if high-pressure forms of sp^3-bonded carbon nitride (C_3N_4) have even a larger bulk modulus than diamond, as theoretically predicted [15]. Reviews on the high-pressure synthesis of ultrahard materials have been recently published [14, 16].

Pressures now available in laboratories can induce changes in the free energy of materials that exceed those of the strongest chemical bonds present at ambient pressure (>10 eV). Therefore, pressure can completely redistribute electronic densities and change the nature of the chemical bonds. In this way, pressure leads to profound changes in materials, like converting insulators into metals and soft chemical bonds into stiff bonds. Furthermore, pressure gives a new dimension to the venerable Periodic Table

since elements under compression develop redefined affinities, electronegativities, and reactivities. In fact, almost all elements, including hydrogen, are theoretically predicted to behave as metals above a certain pressure.

High pressures can be applied to materials in a controlled manner in the laboratory using several devices. Most of them derive from the pioneering work developed by the Nobel laureate Percy W. Bridgman during the first half of the 20th century [17, 18]. Bridgman used mainly cells consisting of two opposed truncated cone-shaped anvils of tungsten carbide (Bridgman-type cell) that squeeze a pyrophyllite chamber containing the samples to be studied [19]. The work of Drickamer, Williamson, and many others also contribute to the development of high-pressure research [20]. In those early days of high-pressure science, pressure-induced phase transitions were usually detected through the sudden changes in resistivity of the squeezed materials and maximum pressures were of the order of 10 GPa. In the post-Bridgman era, a number of other high-pressure apparatus were designed. One of them was the piston-cylinder cell where a sample surrounded by a liquid is closed in a cylinder chamber and pressurized by a piston that is compressed by a hydraulic press [1]. Electrical, magnetic, and optical studies could be performed up to a maximum pressure of 3–4 GPa both at low and high temperatures. However, the major development for the expansion of high-pressure studies was the introduction of the DAC in the two decades following 1950. With this device pressures in excess of 100 GPa (1 Mbar) can be achieved safely since the stored energy is very small due to the small pressurized volume (around 10^{-3} mm^3). To get further details of the high-pressure techniques the reader may consult the book of Eremets [1], the collection of review articles edited by Holzapfel and Isaacs [21], and the collection of review articles edited by Hemley and Mao [22]. In the next paragraphs we will give a brief description of the operation of the most common high-pressure devices used to study pressure-induced phase transitions. A detailed account of them can be found in Refs. [22, 23].

Nowadays, the most common device to provide high pressures in all laboratories is the DAC that was designed by Lawson and Tang [24] and developed by Jamieson et al. [25] and Weir et al. [26]. A DAC is a device consisting of two opposed anvils formed by brilliant-cut, gem-quality diamonds each showing two plane surfaces: the table, with a big area S (≈4 mm), and the culet, with a small area s (50 – 500 μm) (see Fig. 1). When a force F is applied to the table the force is transmitted to the culet resulting in a great pressure, $P = F/s$, due to the small dimensions of the culet. Due to the large hardness of diamond, in a DAC the pressure can be higher than 100 GPa and the highest pressure attained in the laboratory with a DAC is around 400 GPa [27]. In the DAC the pressure is generated axially but it is usually transmitted to the sample quasi-hydrostatically; i.e., in all directions of the sample. The transmission of quasi-hydrostatic pressure to the sample in the DAC is based on the Pascal principle; i.e., the pressure

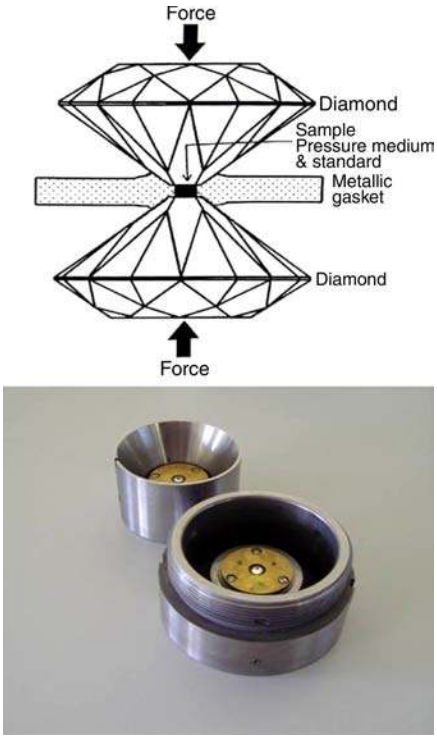

Figure 1 (online colour at: www.pss-b.com) Photograph of the diamond-anvil cell and a schematic view of it.

is transmitted equally to all parts of a fluid in equilibrium. For that purpose, the sample to be pressurized is loaded into a hole performed in a thin metallic gasket (<100 μm in thickness) where the sample is completely surrounded by a pressure-transmitting medium in static equilibrium. When the two diamond anvils, separated by the gasket, squeeze the gasket the metal foil deforms plastically and the dimensions of the hole are reduced thus pressurizing the medium that transmits the pressure quasi-hydrostatically to the sample. A reference material, like a ruby chip, is usually loaded together with the sample in the gasket hole in order to measure the pressure at which the sample is exposed.

Studies of pressure-induced phase transitions using the DAC have been performed using almost all the experimental techniques of condensed-matter physics either at cryogenic or high temperatures or at high magnetic fields. Changes in the structural parameters between two phases can be analyzed by X-ray and neutron diffraction. Changes in atomic coordination can be analyzed by X-ray absorption spectroscopy, or by Mossbauer spectroscopy (if a radioactive atom is present in the sample). Changes in the vibrational properties of two phases depending on the composition and structural symmetry of the material can be analyzed by Raman, Brillouin, and inelastic X-ray scattering and by infrared spectroscopy. Changes in the optical properties can be analyzed by optical absorption or photoluminescence measurements, among other spectroscopic techniques. Finally, the electronic properties can be analyzed by means of electrical and magnetic measurements.

The optical techniques (optical absorption, Raman, and photoluminescence) are the easiest ones to perform high-pressure studies inside the DAC since the diamonds are transparent over a wide range of frequencies from the infrared to the ultraviolet (5.5 eV). However, X-ray powder diffraction is the most commonly used when one wants to know the structure of the different phases because diamonds in the DAC are transparent to hard X-rays exceeding 10 keV. Initially, X-ray studies were conducted in laboratories using X-ray tubes or rotating-anode type sources. These in-house experiments were rather time-consuming due to the low flux of X-rays and the small volume of the scattering sample inside the DAC. However, most of the knowledge of structures at high pressures is posterior to 1980 due to the wide access to high fluxes of X-rays at modern synchrotron sources that enable to perform X-ray diffraction measurements in reasonable times and observing weak peaks at the X-ray diffraction patterns that previously were not measured due to the low flux and small scattering power of some samples. Almost all the high-pressure structures have been analyzed by means of powder diffraction instead of using single-crystal diffraction because many single crystals transform into polycrystals when they suffer a pressure-induced phase transition. Initially, energy dispersive X-ray powder diffraction was used due to the high flux of all X-ray energies incoming in the DAC; however this method yields poor resolution and suffer a number of disadvantages including the contamination of spectra with fluorescence lines from the sample. Nowadays, angle-dispersive X-ray diffraction measurements are preferred despite their smaller flux compared to energy dispersive measurements due to the development of image-plate detectors that record ring two-dimensional X-ray patterns. Image-plate detectors offer high intensity by integrating the two-dimensional pattern and good resolution that enable Rietveld refinement of the high-pressure structures. Similarly to X-ray powder diffraction, neutron powder diffraction is used to resolve the structure in compounds with light elements showing small X-ray scattering factors. However, due to the smaller flux of neutrons one needs larger quantities of sample and the use of miniature DAC is replaced by large volume presses (LVP), like the Paris–Edinburgh cell. The highest pressure achieved with a LVP is limited to around 60 GPa [28]. The Paris–Edinburgh cell is a modified version of the Bridgman-type cell which is designed to be placed at the exit of the neutron flux of a nuclear reactor or a neutron spallation source [29]. In essence, the Paris–Edinburgh cell is a device in which a powder sample is compressed between two opposed anvils made of either tungsten carbide or sintered diamond. Sample confinement is achieved by means of a null-scattering gasket with toroidal rings, which locate into corresponding grooves machined in the anvil profile. Application of pressure is then achieved by means of an in-situ hydraulic ram, which can apply loads of up to 250 tonnes between the two anvils.

Sometimes the analysis of neutron or X-ray powder diffraction patterns is not enough to clearly resolve the structure of a high-pressure phase. In this respect, theoretical calculations and other experimental techniques, like X-ray absorption, X-ray emission, Raman scattering and photoluminescence, can be of valuable help. Notably, many beamlines of modern synchrotron sources dedicated to X-ray diffraction studies at high pressures now include the possibility to record Raman scattering together with the X-ray diffraction patterns. Additionally, advancements in theoretical calculations due to the increase of computer power and the development of efficient algorithms especially in density-functional theory in the last two decades have lead to total-energy quantum mechanical calculations of the stability of different atomic arrangements in an ever increasing number of compounds [30]. Recent measurements in scheelite tungstates have highlighted the importance of combination of X-ray diffraction measurements, X-ray absorption studies, Raman scattering measurements, and first principles calculations to help in the exact determination of complex diagrams of high-pressure phases in ABX_4 compounds [31–34].

In the next section we describe the main characteristics of solid–solid pressure-induced phase transitions. We highlight the most relevant phase transition features found in a number of different inorganic compounds giving an overview of the state of the art in high-pressure research by emphasizing recent discoveries, hot spots, controversial questions, and future directions of research. A brief update of previous reviews of oxide and orthosilicate minerals [35–37] is given. The description of magnetic, electronic, optical, elastic, and mechanistic aspects of solid–solid phase transitions are out of the scope of the present Feature Article.

2 High-pressure phase transitions in elements and inorganic compounds At given conditions of temperature, pressure, and composition, matter is characterized by an arrangement of atoms with determined intrinsic properties, that we call phase. When the interatomic distances of compressed matter are reduced, the forces between the atoms are modified and the Gibbs free energy of the atomic arrangement changes. Usually, the Gibbs free energy of the stable atomic arrangement of a material at certain pressure (phase 1) increases with increasing pressure. Therefore, at a certain pressure there could be a different atomic arrangement (phase 2) with a smaller Gibbs free energy than that of the pressurized phase 1. At this pressure, the atomic arrangement of the material in phase 1 is unstable against the new atomic arrangement of phase 2 and it is favorable for the material to change the atomic arrangement to minimize the Gibbs free energy at those conditions. When at a certain pressure a material suddenly changes the symmetry of its atomic arrangement from that of phase 1 to that of phase 2 it is said that the material has suffered a pressure-induced phase transition. This transition to a new structure is usually accompanied by an in-

crease in the density of the material and new materials can be obtained when the new structure of pressurized materials can be retained on decreasing pressure to ambient pressure; i.e., when the new structure is quenched at ambient conditions.

Phase transitions can be classified according to their thermodynamic order, which is the order to the derivative of the Gibbs free energy, G, what first show a discontinuity. A pressure-induced phase transition is said to be of first-order when it exhibits a discontinuity in the first derivative of G with respect to the variable pressure, P. A pressure-induced phase transition is said to be of second-order when it has a discontinuity in a second derivative of G with respect to P. Since the derivative of the Gibbs free energy with respect to pressure at constant temperature is the volume, $\delta G/\delta P = V$, a pressure-induced first-order phase transition shows an abrupt change in the unit cell volume between the two phases. On the other hand, since the second derivative of G with respect to P is proportional to the compressibility, pressure-induced second-order phase transitions do not show a change in the unit cell volume between the two phases but a discontinuity in the compressibility of the two phases. Experimentally it is sometimes very difficult to distinguish a weak first-order phase transition from a second-order phase transition. However, the symmetry changes in second-order phase transitions can be traced by group-theoretical methods based in the Landau theory of phase transitions that have been recently reviewed [38–40].

On the other hand, the solid–solid phase transitions can be classified as displacive or reconstructive from the structural point of view. A displacive or diffusionless phase transition do not occur by the long-range diffusion of atoms but rather by some form of cooperative, homogeneous movement of many atoms that results in a change in crystal structure often accompanied by a small strain. The atomic movements are small, usually less than the interatomic distances, and the atoms maintain their relative relationships. In this case, the two structures or phases usually obey to a group-subgroup relationship and the atomic bonds of the parent phase do not break at the phase transition. On the contrary, a reconstructive or diffusive phase transition takes place when atoms are diffused from their original sites moving through distances longer than interatomic distances. In a reconstructive phase transition atomic bonds are broken to form new bonds and the two phases do not have the need to obey a group-subgroup relationship. First-order phase transitions can be either of reconstructive or displacive type while second-order phase transitions are of usually displacive type and occur via the "soft mode" mechanism, in which the frequency of a vibrational mode or a volume-preserving shear mode goes to zero. Additionally, pressure-induced second-order phase transitions show no major change in cation coordination and are usually reversible; i.e., the initial phase is recovered after pressure release. However, first-order phase transitions are usually accompanied with an increase in cation coordination and are irreversible or show a relatively large hysteresis (difference in the phase transition pressure at increasing and decreasing pressure) when the transition is reversible.

A reconstructive phase transition usually yields different phase-transition pressures on increasing pressure or decreasing pressure. This hysteresis is especially large in first-order reconstructive phase transitions of covalent materials which are usually characterized by large kinetic barriers that impede the transition at the equilibrium pressure of the two phases. That is the case of diamond that it is theoretically predicted to transit from the graphite structure to the diamond structure at 1.7 GPa at room temperature (RT), but the phase transition is hindered by a large kinetic barrier that is overcome only at high pressures and temperatures (5–9 GPa and 1200–2800 K) [30]. In these cases, the true experimental equilibrium thermodynamic pressure must be considered to be located at the middle of the hysteresis interval. It is this experimental pressure what can be compared to the calculated equilibrium pressure of the two phases obtained from theoretical calculations that do not take into account the kinetic barriers. Furthermore, when different techniques study the same reconstructive phase transition each technique could yield a different phase-transition pressure. For instance, usually photoluminescence and Raman scattering measurements give the smaller pressure values, X-ray absorption measurements give intermediate values, and X-ray diffraction measurements tend to give the larger values. The reason for the differences in the estimation of the phase transition pressure with different techniques is due to the local or non-local character of the different techniques. The merits of the different methods for locating the thresholds of reconstructive phase transitions have been already discussed in the literature [33, 41].

It is well known that the density of materials of given families in the Periodic Table tends to increase with the atomic number of their constituents and that applying pressure tends to reduce these differences. In fact, even soft materials with van der Waals forces at ambient pressure become stiff at high pressures. The increase in density is due to the overall decrease of the interatomic distances with increasing pressure; however, pressure also leads to a decrease of the atomic size. In this respect, it is empirically known that long bonds are usually softer and more compressible than short bonds; and that anions (which have large ionic radii) are usually more compressible than cations (which usually have small ionic radii) [42, 43]. On the light of these considerations the effect of pressure is twofold: (i) with increasing pressure the decrease of the interatomic distances and of atomic sizes leads to an increase of the cation–cation repulsive forces [44, 45]; and (ii) the large reduction of anion sizes compared to cation sizes leads to an increase of the packing efficiency of anions in the cationic sublattice. Therefore, applying pressure results in: (i) an increase in density of materials, (ii) an increase of cation coordination, and (iii) a decrease of compressibility of the material due to electronic repulsion between cations.

On the basis of the above considerations, all pressure-induced phase transitions have some common features. On one hand, pressure-induced phase transitions are characterized by dense atomic arrangements where all atoms tend to increase their coordination provided that cation–cation repulsive forces are small enough to allow that a new crystalline phase is formed. This is the so-called "pressure-coordination" rule. Another rule, the so-called "corresponding state principle", stays that atomic arrangements at high pressures of compounds with light elements are those observed in analogous compounds with heavy elements at smaller pressures. This means that for instance elements of the same group in the Periodic Table tend to adopt similar structures at high pressure. A clear example is given by group-IV elements (C, Si, Ge, and Sn). Carbon crystallizes in the hexagonal graphite structure at ambient pressure and undergoes a pressure-induced phase transition to the diamond structure (which is the structure of Si and Ge at ambient pressure), while Si and Ge undergo a pressure-induced phase transition to the β-Sn structure (that of Sn at ambient pressure). This idea implies that it is possible to construct generalized phase diagrams for the different elements and compounds and consequently that it is possible to understand the systematic of pressure-driven phase transitions of materials.

A paradox of pressure-induced phase transitions is that despite high-pressure phases have usually higher density (smaller volume) and higher atomic coordination than low-pressure phases, the increase in coordination is correlated to an increase in the interatomic distances. For example, the C–C distance in graphite is 1.42 Å while in diamond is 1.54 Å. Note that the effect of pressure in a certain crystalline structure is to reduce the overall interatomic distances; however, once the phase transition from a low-pressure phase to a high-pressure phase is accomplished the interatomic distances in the new phase can be larger than in the old one despite having the new phase a more compact structure with smaller unit cell volume. In the following we will revise the main high-pressure phase transitions in several inorganic compounds of different families; i.e., with different stoichiometry.

2.1 Elements under pressure A number of reviews have been devoted to the pressure-induced phase transitions in the different elements under pressure in 1972 [46], 1976 [47], 1986 [37], 1991 [48], 2004 [49] and 2005 [50]. More recently a review of the behavior of the metallic elements (except actinides and lanthanides) under high pressure has been published [51]. Many non-molecular elements crystallize in simple high-symmetry structures at ambient pressure and temperature like the body-centered cubic (bcc), face-centered cubic (fcc), or hexagonal close-packed (hcp) structures. In general, they undergo phase transitions under pressure to denser phases with more close-packed structures and increasing atomic coordination, except alkaline and alkaline-earth elements due to the promotion of s- and p-electrons to d-orbitals with increasing pressure [52, 53]; however, due to the considerable differences of the electronic configurations in the different elements very different high-pressure phases including complex incommensurately modulated and incommensurate host-guest composite structures have been discovered in the last two decades. It is worth mentioning that despite considerable progress has been recently made in determining the crystal structures of the complex high-pressure structures [54], little is known about their physical properties [55]. In fact, an unexplored area for searching a charge-density wave state competing with the superconducting state in many complex incommensurate crystal structures of group V, VI, and VII heavy elements has been recently devised [56]. Furthermore, the observation of crystal-chemical differentiation of physically identical atoms in several complex high-pressure modifications of some metallic elements has encouraged renewed interest in the properties of compressed binary alloys [49]. This crystal-chemical differentiation of otherwise identical atoms may be related to the proposed charge transfer of electrons to the lattice in order to satisfy the "8-N or octet" rule for electronic configurations [57]. Figure 2 shows the Ba-IV structure that constitutes an example of the incommensurate structures (composed of a host and several guest structures). The Ba-IV phase is isostructural to $K_{0.42}Cd_2$ and to the Bi_2Al_2 squeleton in $Bi_2Al_2O_9$. This last structure has been interpreted in Ref. [58].

Special attention must be given to the phase transitions of group 14 (or group IVA) elements because: (i) they are related to III–V and II–VI semiconductors; (ii) they are key to understand the phase transitions in a number of complex compounds, and (iii) they display recently developed framework structures with unusual properties. The phase transitions of group 14 elements have been recently reviewed [30, 59]. The stable form of C under normal conditions is hexagonal graphite which transforms into diamond at high pressures and temperatures as already com-

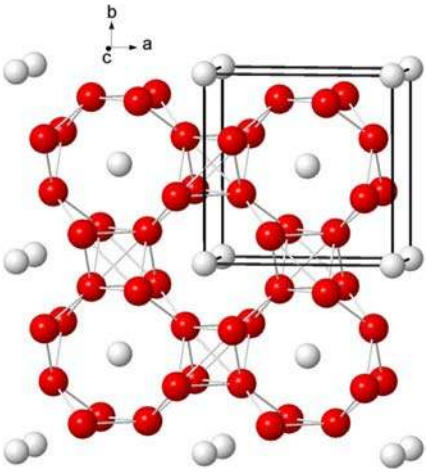

Figure 2 (online colour at: www.pss-b.com) Incommensurate Ba-IV structure showing both the host (red) and guest (white) structures.

mented. In diamond, C atoms are fourfold-coordinated and the diamond phase is metastable at ambient conditions; however, it has been theoretically predicted to undergo a transition to a sixfold-coordinated structure at pressures of the order of 1 TPa, which is far beyond the pressures already obtained in the laboratory (see discussion in [30]). Furthermore, despite diamond is an electrical insulator at ambient conditions, boron-doped diamond synthesized at high pressure and high temperature has been found to be a low-temperature superconductor [60]. This discovery suggests that Si and Ge, which also crystallize in the fourfold-coordinated diamond structure, may similarly exhibit superconductivity under appropriate conditions. Si and Ge undergo phase transitions to the β-Sn, Imma, simple hexagonal (sh), Cmca, and hcp structures. A further hcp to fcc transition has been experimentally observed in Si, which is stable up to the highest pressure reached (248 GPa [61]), but has not been found in Ge up to the highest pressure reached (190 GPa [62]). All these phase transitions are accompanied of an increase in atomic coordination with increasing pressure. Interestingly, several phases have been found in Si and Ge on decreasing pressure from the β-Sn phase. Bc8 or r8 phases have been found in Si, while bc8 or st12 phases have been found in Ge depending on the slow or rapid decrease of pressure or the temperature. As regards Sn, it is a semimetal that crystallizes at normal conditions in the β-Sn structure and transits to structures with higher atomic coordination, first to the bct phase and afterwards to the bcc phase, which is stable up to at least 120 GPa [63]. A transition at higher pressures to the hcp phase has been theoretically predicted [64]. Finally, Pb is a metal that crystallizes at normal conditions in the fcc structure. A first phase transition to the hcp and a second phase transition to the bcc structures have been reported [65, 66].

The most recent developments in group 14 elements are the formation of expanded framework allotropes of C, Si, Ge, and Sn. At ambient conditions carbon can be crystallized in expanded forms containing nano-sized cages. Some of them are closed structures named fullerenes, C_{60} or C_{70}, which can be linked to form fullerites through van der Waals bonds between the cages; others are open structures known as nanotubes. For a detailed account of the properties of fullerites under pressure we refer the reader to recent reviews [67–69]. Expanded forms of Si, Ge, and Sn are collectively known as clathrates. Studies in group 14 clathrates and their high-pressure behaviors have been recently reviewed [69–71]. Some of them are superconducting, like silicon-based Ba-doped clathrates [72, 73], and are often prepared under high-pressure conditions or even theoretically predicted to be stable at negative pressures like clathrate Si_{136} [74].

Actinides and lanthanides have also an interesting high-pressure behavior, particularly because of the role played by f-electrons. The nature of the 4f electrons in many rare-earth metals and compounds may be broadly characterized as being either "localized" or "itinerant," and it is held responsible for a wide range of physical and chemical properties. The regular trivalent rare-earth structural sequence [75–77] observed at low pressures for La through Lu excepting Eu and Yb as a function of increasing pressure or decreasing atomic number, typifies this behavior. All of them are high-symmetry close-packed structures and the sequence hcp → Sm-type → double hexagonal close packed (dhcp) → fcc may be reproduced solely by transfer of sp electrons to the d-band [52]. The same sequence is observed under pressure in 4d metal Y, which has no adjacent f-states. Under further compression, the 4f electrons become itinerant, fully participating in chemical bonding. This leads to open, low-symmetry structures. The transition is of first order and may be accompanied by a discontinuous drop in volume and a stiffening of the crystalline lattice. Examples of these structures are the α-U (Cmcm) structure and the monoclinic C2/m structure found in Gd, Tb, and Pr [78–81]. In the case of the actinides, these 5f elements show many high-pressure properties which have direct correspondence to the 4f lanthanides. A detail description of their high-pressure behavior has been given by Johansson and Li [82].

2.2 AX compounds Similarly to the case of the elements under pressure, two relatively recent reviews have been devoted to the high pressure phase transitions in AX compounds, especially for the important binary semiconductors of the III–V and II–VI families present in the optoelectronic industry [30, 59]. The less ionic of these binary semiconductors crystallize in the zincblende ($F\bar{4}3m$) structure, like AlSb, AlAs, AlP, GaSb, GaAs, GaP, InSb, InAs, InP, ZnS, ZnSe, ZnTe, CdS, CdSe, CdTe, HgS, HgSe, and HgTe. Some binary semiconductors with a certain ionic character crystallize in the wurtzite ($P6_3mc$) structure, like AlN, GaN, InN, ZnO, and BeO. Finally, the most ionic binary semiconductors (MgO, CdO, HgO) and most of the binary alkali halides (I–VII family) crystallize in the rocksalt ($Fm\bar{3}m$) structure. Since rocksalt-structured alkali halides transit to the CsCl ($Pm\bar{3}m$) structure, the sequence of pressure-induced phase transitions expected for the zincblende compounds was: zincblende → rocksalt → double β-Sn → CsCl [83]. However, zincblende binary semiconductors either undergo a phase transition to the rocksalt or to the Cmcm phase (an orthorhombic distortion of rocksalt) while the double β-Sn structure is not observed in any IIIA–VA and IIB–VIA compound [30].

An unexpected structure found in these compounds is the hexagonal cinnabar ($P3_121$) phase with cation coordination between that of the zincblende and of the rocksalt phase. The cinnabar structure can be considered as a distortion of the Si subarray in quartz and is related to the structure of the alloy $CrSi_2$ [58, 84]. In fact, the formation of the cinnabar structure by Si atoms in quartz agrees with the relationship established between oxidation and pressure [85, 86]. When O atoms are inserted into the Si network, the Si atoms "feel" the pressure and stabilize the high-pressure Si structure (cinnabar-like). This pressure can be

released by heating and consequently quartz transforms at high temperature into cristobalite where the ambient pressure (diamond-like) structure of Si is recovered. The sequence expected under pressure for III–V and II–VI compounds is zincblende → cinnabar → rocksalt → Cmcm → CsCl. In fact, ZnTe follows the sequence: zincblende → cinnabar → Cmcm. HgS crystallizes in the cinnabar phase at ambient conditions and undergoes a phase transition to the rocksalt phase near 13 GPa [87]. The absence of the high-pressure rocksalt phase (in some compounds like GaAs) and the direct transition to the Cmcm phase is related to the ionicity of the compounds, being the most ionic those that exhibit a larger tendency towards the rocksalt phase [88]. The absence of a phase transition towards the CsCl phase at even higher pressures in many compounds has been also theoretically discussed [89, 90]. Recently, a theoretical review of the predicted phases of InAs under high pressure above the Cmcm structure, and giving support to a super-Cmcm structure, has been published [91]. Also a review of the high-pressure phases in II–VI semiconductors has been recently published [92]. We have to comment that the mechanism of the above transitions is still not clear and seems to depend on the material. The mechanisms of the first-order zincblende-to-rocksalt and wurtzite-to-rocksalt phase transitions have been recently discussed in a number of compounds (see Refs. [93, 94] and references therein).

A particular mention in this section deserves the alkaline-earth chalcogenides (AX with A = Be, Mg, Ca, Sr, Ba and X = S, Se, Te). These semiconductors have important applications in optoelectronic devices specially when mixed with II–VI wide band gap semiconductors. Pressure-induced phase transitions from octahedrally-coordinated structures to eightfold-coordinated structures are very common in these compounds [95–98]. A very interesting feature is that compression leads to a gradual overlap of the valence band with the conduction band which causes a metallization of the compounds, in some cases at relatively low pressure like in BaTe where the metallization occurs at 20 GPa. Most of them, like MgS and MgSe, crystallize in the rocksalt structure but some of them, like MgTe, crystallizes either in the wurtzite or NiAs structures despite the hexagonal NiAs ($P6_3/mmc$) structure has been predicted to be the most stable at ambient pressure [99]. In fact, a wurtzite to NiAs phase transition was found between 1 GPa and 3.5 GPa [100]. Recently, a theoretical prediction of the phase transition from the NiAs structure to the orthorhombic Pnma structure above 43 GPa has been published [101] despite no transition was found up to 60 GPa [100]. On the other hand, MgSe has been found to transit from the rocksalt to the FeSi structure around 100 GPa in relatively good agreement with calculations [102, 103].

Especially important to Earth sciences is the monoxide group, which includes simple oxides of the divalent metals. At least thirty monoxide minerals and compounds are known, with two thirds crystallizing in the cubic rocksalt structure. Some of these oxides like periclase (MgO) and wustite (FeO) have been the subject of extensive high-pressure studies due to their geophysical relevance [104–106]. The rocksalt structure is found to remain stable up to Mbar pressures. However, a phase-transition to the CsCl structure is predicted. The NaCl to CsCl phase transition is very well-known in NaCl [107] and has been found to take place in other alkali halides [108], and also in some silver halides [109, 110]. In particular, it has been also experimentally found in other alkaline-earth oxides like CaO at relative low pressure [111]. The rocksalt-to-CsCl phase transition always occurs with a large volume collapse indicative of its first-order nature. Notably, copper halides and AgI, which are less ionic I–VII compounds, crystallizes either in the zincblende or in the wurtzite structures and undergo a phase transition towards the rocksalt phase [112, 113]. In the case of AgI, an intermediate structure between NaCl and CsCl has been recently proposed to be to either a monoclinic $P2_1/m$ or to orthorhombic Cmcm [113] but still has to be experimentally confirmed.

2.3 A_2X compounds Among these compounds the A_2O materials are the most studied under high pressure. Due to the –2 valence of O, the A cation should have valence +1 and this limits the number of compounds with this stoichiometry to alkaline cations plus H, Cu and Ag. H_2O is the most studied A_2X compound because of its paramount importance in the physical and chemical sciences and its key role in life. Water is a molecular compound with important hydrogen bonding that freezes with increasing pressure and whose pressure-temperature phase diagram shows a large number of different liquid and solid phases (ices) with many unresolved questions [114–118].

Related to H_2O is Li_2O which has been recently studied upon compression [119, 120]. A pressure-induced phase transition from the cubic antifluorite (Fm3m) to the orthorhombic anticotunnite structure (Pnma) apparently takes place at pressures between 45 GPa and 50 GPa (experiment) or at 36.9 GPa (first-principles calculations). The anticotunnite structure has been observed also in Li_2S, Na_2S, and K_2S under pressure [121–123] and has been proposed as a new high-pressure phase of ice above 150 GPa [124, 125]. Furthermore, sulfides undergo a pressure-induced phase transition from the anticotunnite to the hexagonal θ-Ni_2In structure ($P6_3/mmc$) and it has been predicted that this will occur also in Li_2O above 100 GPa [126] and likely in the other alkaline oxides (Na_2O, K_2O, Rb_2O, and Cs_2O) for which interesting theoretical predictions have been made [127]. Interesting for the future is also the high-pressure study of antifluorite compounds like Mg_2X (X = Si, Ge, Sn) and Be_2C which are expected to contribute to the better understanding of the structural behavior of ionic A_2X compounds.

The crystal structure of cuprite (Cu_2O) and its isomorph, Ag_2O, is cubic (Pn3m) with Cu or Ag at the 2a position and O at the 4b position. In this structure the cations have an unusual linear two-coordination, where each O is

coordinated to a tetrahedron of Cu or Ag cations. Cu_2O transforms to a hexagonal structure at 10 GPa and to the $CdCl_2$ (R32) structure at 18 GPa [128]. In Ag_2O the hexagonal structure becomes stable at 0.4 GPa and it is retained at least up to 29 GPa [128]. At high temperature (450 °C) cuprite decomposes into Cu + CuO but such a breakdown has not been observed upon compression.

To close this section we would like to call the attention of the readers to silicides like Ni_2Si and Fe_2Si, which have been recently studied under compression [129], and are important because the Earth's core is believed to consist of an iron-nickel alloy with several percent of light alloying elements. For Fe_2Si, two different polymorphs have been reported in the literature, the cubic hapkeite structure ($Pm\bar{3}m$), found in grains of lunar meteorites, and a trigonal structure ($P\bar{3}m1$), which is a slight distortion of the Ni_2Al-type structure. The recent studies showed that the last structure is the most stable structure and that it is expected to remain stable up to Mbar pressures. They also found that Fe_2Si has a bulk modulus of 255 GPa, the largest value found among iron silicides. This hardness seems to be related with the high Si–Fe coordination; each Si is coordinated by 11 Fe atoms. Regarding Ni_2Si, at ambient conditions it crystallizes in an orthorhombic structure (Pbnm) but at high temperature it transforms into the hexagonal θ-Ni_2Si, an aristotype of θ-Ni_2In. However, upon compression the orthorhombic structure of Ni_2Si is theoretically predicted to be stable up to at least 400 GPa [129]. It is important to note here that a highly anisotropic compression was observed in Ni_2Si. In particular, the linear incompressibility of Ni_2Si along the *c*-axis is similar in magnitude to the linear incompressibility of diamond. This fact is related to the higher valence-electron charge density of Ni_2Si along the *c*-axis and could lead to future industrial applications of Ni_2Si.

2.4 AX_2 compounds The pressure-induced phase transitions in AX_2 compounds have been reviewed in Ref. [130]. Silica (SiO_2) is by far the most important AX_2 compound for fundamental solid state physics and chemistry and for Earth and materials science. Silica exhibits a very rich polymorphism with more than 30 stable or metastable structures, depending on the pressure–temperature history of the samples studied; and some of the silica phases are abundant in nature, like α-quartz and stishovite. Therefore, the stable form of silica at ambient conditions (α-quartz) is a model material for studies of chemical bonding, structural phase transitions, glass formation, and mineralogy.

The majority of the polymorphs of silica observed at pressures below 9 GPa, like quartz, high and low cristobalites, tridymites and coesite, are built of SiO_4 tetrahedra [131, 132]. Denser forms of silica, like stishovite, the monoclinic $P2_1/c$ phase, the $CaCl_2$-type, and α-PbO_2-type phases, containing SiO_6 octahedra, are formed above 9 GPa [132–136]. Among the high-pressure phases of silica, rutile-type SiO_2, also known as stishovite, is the most important because is one of the main components of the Earth's mantle. Therefore, the high-pressure behavior of rutile-type dioxides is of considerable importance to mantle mineralogy.

In addition to silica other important AX_2 compounds are rutile (TiO_2) and its isomorphs, which display a tetragonal symmetry ($P4_1/mmm$). They represent the most common structure of naturally occurring AO_2 dioxides. Rutile is the ambient structure of cassiterite (SnO_2), pyrolusite (MnO_2), plattnerite (PbO_2), germanium dioxide (GeO_2), and ruthenium dioxide (RuO_2). In the rutile structure, the oxygen sublattice can be seen as a largely distorted fcc in which only one of the two octahedral sites is filled by the metal. The rutile structure has been also shown to consist of infinite rectilinear chains of AO_6 octahedra parallel to the *c*-axis, united by corner sharing to the identical adjacent chains. This arrangement of octahedral chains causes the highly anisotropic structural compression and thermal expansion. High-pressure studies of rutile-type dioxides have shown that they have large axial compression anisotropy with the *a*-axis being twice as compressible as the *c*-axis [137, 138]. This can be attributed to the strong metal cation–cation repulsion along the edge sharing chains of octahedra. It is noteworthy that these compounds are quite uncompressible with a bulk modulus ranging from 216 GPa (TiO_2) [139] to 313 GPa (SiO_2) [134].

In addition to rutile, there are several other dense forms of AO_2 dioxides because comparable energies are found for slightly different octahedral interlinks. For example six polymorphs have been reported in PbO_2 at pressures lower than 47 GPa [140]. GeO_2 undergoes a transition at RT from the tetragonal rutile structure at ambient pressure to the cubic pyrite-type structure ($Pa\bar{3}$) at 70 GPa [141], following the structural sequence: rutile → $CaCl_2$-type (Pnnm) → α-PbO_2-type (Pbcn) → pyrite. This transition sequence is the same as that in SnO_2 and RuO_2 [142, 143]. Furthermore, studies in SiO_2 showed the same transition sequence except for the pyrite phase [144]. The pyrite structure is basically a modified fluorite structure with the oxygen atoms significantly displaced from their positions in the fluorite structure. This leads to a distortion of the coordination polyhedron from a cube to a regular rhombohedron resulting in an increase of the Si coordination from 6 in rutile to 6 + 2 in pyrite. High-pressure studies have been also carried out in ZrO_2 (baddeleyite), HfO_2, CeO_2, and TiO_2 [145–150]. In these compounds, the α-PbO_2-type, fluorite-type (Fm3m), baddeleyite ($P2_1/c$) and cotunnite (α-$PbCl_2$) structured phases become stable upon compression. Recently discovered new phases of TiO_2 have promising properties. Cotunnite-type TiO_2 (see Fig. 3) is the hardest oxide known [151] and the cubic phase of TiO_2 (c-TiO_2), synthesized at a pressure of 48 GPa and temperatures of 1900–2100 K by heating anatase in a DAC [152], could be an important material for future generation of solar cells because it has an absorption coefficient in the visible range 3 or 4 orders of magnitude larger than the anatase TiO_2 used in conventional solar cells. However, the exact nature of the promising cubic TiO_2 (c-TiO_2) phase,

with either the fluorite or pyrite structure, still has not been solved [153]. In all these compounds, the high-pressure phases have a smaller compressibility than the rutile phase; e.g. the bulk modulus of rutile phase in TiO_2 is 216 GPa while in the α-PbO_2 phase is 253 GPa [149]. This fact is consistent with the increase of the Ti coordination induced by pressure. It is interesting to mention here that the combination of pressure and temperature create a very rich polymorphism for the AO_2 compounds, in particular in SiO_2 and GeO_2. In these two dioxides, apparently kinetics has a large effect on pressure-induced phase transitions. Therefore, the high-pressure behavior of SiO_2 and GeO_2 depends on the starting material and the pressure-temperature history [154]. However, it has been shown that both dioxides have a common sequence of high-pressure high-temperature structural transformations [154]. Most important, the end-stage of the structural sequence is in both cases the pyrite-type structure, reached in GeO_2 at 70 GPa and in SiO_2 at 205 GPa. In spite of the large amount of theoretical and experimental work already carried out on AO_2 compounds, the study of pressure-driven phase transitions in them down to the core-mantle boundary of Earth needs further analysis because it can affect the lower mantle composition through a possible breakdown of silicate perovskite, the major lower mantle mineral.

An interesting case is that of TeO_2 which is the only oxide showing a post-cotunnite phase whose structure is not known. The post-cotunnite phase seems to be neither the Ni_2In nor the Co_2Si found in some dihalides at high pressures [155]. Possible phases for this structure might be the Ca_2Si ($P2_1/c$) structure also found in $BaCl_2$ and $PbCl_2$ [156, 157] or the $MgCu_2$ ($Fd\bar{3}m$) of cubic Laves structure, which is also observed in the cation substructure of spinels. As regards the high-pressure behavior of compounds that crystallize in the cubic Laves structure ($MgCu_2$-type), $CeAl_2$ and $GdAl_2$ are found to be stable in the cubic Laves phase up to 23 GPa and 16 GPa, respectively [158]. However, these compounds have been predicted to transform to the hexagonal $MgZn_2$ Laves structure ($P6_3/mmc$) [158]. Recent studies on YFe_2, $ErFe_2$ and YMn_2 found that the Laves phases retained their initial cubic structure at least up to 30 GPa [159, 160]. In the case of UMn_2, according with X-ray diffraction experiments, the cubic Laves phase distorts at pressures above 3 GPa. The analysis of the associated splitting of the diffraction lines reveals that this distortion is orthorhombic and qualitatively the same as the already known distortion observed at low temperatures [161]. It is also interesting to note that in the structural map for AX_2, the compound $ThAl_2$, which crystallizes in the AlB_2 structure at ambient conditions, falls upon moderate compression in the region of Laves phase ($MgCu_2$) compounds [162]. The study of the high-pressure behavior of Laves structures has recently received a lot of attention because recent studies on $CaLi_2$ have predicted that it should be a very peculiar material under pressure. Its structure is predicted to undergo a structural bifurcation on densification to structures compressed or elongated in one lattice direction [163].

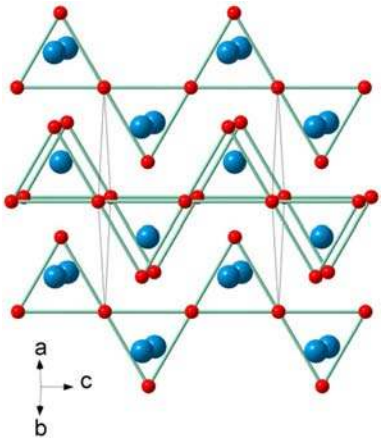

Figure 3 (online colour at: www.pss-b.com) Post-cotunnite phase (hexagonal Ni_2In) in many A_2O and AO_2 compounds. Big blue atoms are In and small red atoms are Ni.

A parallelism can be drawn between the high-pressure behavior of dioxides and difluorides. Most cubic fluorite-type difluorides including CaF_2, CdF_2, SrF_2, BaF_2, MnF_2, PbF_2, and EuF_2 have been shown to transform to the cotunnite (α-$PbCl_2$) structure at pressure below 10 GPa [164, 165]. On top of that, rutile-type MnF_2 was found to transform above 3.6 GPa to the α-PbO_2 phase. This phase trasition is believed to proceed via fluorite-related structures or a cotunnite-type structure [166]. The cotunnite structure is also the high pressure phase of actinide dioxides like UO_2 and ThO_2 which at ambient pressure crystallize in the fluorite structure [167]. Both in oxides and fluorides the transition to the orthorhombic α-$PbCl_2$-type or α-PbO_2-type structures takes place together with a large volume collapse indicative of the first-order character of the transition. The analogies drawn in the literature between oxides and fluorides can be also used to predict the high-pressure behavior of novel compounds like Yb_2Ge, Eu_2Ge, and Eu_2Si, which crystallize in the α-$PbCl_2$-type structure at ambient conditions [168]. Upon compression these compounds quite likely will transform to a structure related to pyrite.

Other compounds like $CaCl_2$ have a slightly different behavior upon compression. It undergoes a sequence of phase transitions which is unique among AX_2 compounds: it transforms from $CaCl_2$ (a monoclinic distortion of rutile) to cotunnite, successively through α-PbO_2, EuI_2 and SrI_2-type phases. In a narrow pressure range, five different phases are found. No other AX_2 compound undergoes such a large variety of transitions, except PbO_2 [169]. In this sequence of transitions the coordination number gradually increases from 6 at ambient pressure to 9 in the cotunnite structure. In this compound, apparently the cubic pyrite-type structure does not become stable upon compression. It is important to note here that the occurrence of the EuI_2 and baddeleyite structures is not frequent in AX_2 compounds. It is found for ZrO_2, HfO_2 and EuI_2 at ambient

pressure or for $CaCl_2$, $CaBr_2$ and TiO_2 under pressure. This structure is only found for compounds with cations which have a particular electronic structure: an empty d-electron shell close to other occupied states [130].

Additional high-pressure studies on AX_2 compounds have been performed in dihydrides and diborides. Rutile-type MgH_2 was examined up to 57 GPa at RT. It was found to transform to γ-MgH_2 with the α-PbO_2 structure [170]. A complete conversion to the γ-phase, however, did not take place and these two phases coexisted up to 9 GPa. Above 9GPa, MgH_2 transformed to an orthorhombic phase (HP1-phase), and further to another orthorhombic phase (HP2-phase) at around 17 GPa. Space groups of the HP1 phase and the HP2-phase were concluded to be $Pbc2_1$ and Pnma (cotunnite-type), respectively. Cotunnite-type MgH_2 was stable at pressures up to 57 GPa. Thus the structural sequence of MgH_2 involves an increase in the coordination number of magnesium ions from 6 to 9. BaH_2 have shown a phase transformation from the cotunnite to the θ-Ni_2In structure at 2.5 GPa, and a second transition between 50 GPa and 65 GPa [171]. At the second transition the arrangement of the cation sublattice changes from an hcp to a sh lattice which seems to be a final step in the structural sequence of ionic AH_2 compounds under high pressure. TiH_2 has also recently revealed a cubic ($Fm\bar{3}m$) to tetragonal (I4/mmm) phase transition at 2.2 GPa which persists up to 34 GPa [172]. It has been also found that the bulk modulus of TiH_2, 146(14) GPa, is greater than that of pure Ti metal, 117(9) GPa [173]. Interstitial alloys of transition metals and hydrogen usually exhibit properties which are unlike those of elemental metals, including crystal structure, mechanical properties, as well as very different electronic properties [174]. In the case of TiH_2, it was found that the binding energy of Ti is greater than that of Ti in the elemental metal, what could account for the greater bulk modulus of the hydride. A similar phenomena has been also observed in MgH_2, which has a bulk modulus close to 55 GPa [175] while Mg has a bulk modulus of about 36 GPa [176].

In this section we would also like to dedicate some space to the important family of diboride superconductors. X-ray diffraction measurements in MgB_2 compressed at RT to 40 GPa did not reveal any phase transformation [177]. However, an anomalous high-pressure behavior has been seen in Raman measurements in MgB_2 near 18 GPa [178] that electronic-structure calculations have assigned to an electronic topological transition. On top of that, indications of a phase transition in MgB_2 above 9 GPa at RT after stress relaxation by laser heating [179] have been observed. The transition was detected using Raman spectroscopy and X-ray diffraction [180]. The structure of MgB_2 (P6/mmm) is composed of planar hexagonal arrays of B atoms intercalated by Mg atoms such that each Mg atom has 12 B atoms in equal distance as nearest neighbors, while each B is surrounded by six equidistant Mg atoms. The observed pressure-induced changes are consistent with a second-order structural transition involving a doubling of the unit cell along the *c*-axis and a reduction of the B site symmetry. Moreover, Raman spectra suggest a reduction in electron–phonon coupling in the slightly modified MgB_2 structure consistent with the previously proposed topological transition in MgB_2. Regarding compressibility, MgB_2 has been found to have a bulk modulus of 150 GPa [181], being this compound also characterized by a moderately sizable anisotropy of compressibilities, which is smaller than for other related diborides like TiB_2 and AlB_2 [182]. An interesting compound is ReB_2 which has been proposed to be a superhard material with an axial compressibility along the *c*-axis smaller than that of diamond [183]. The structure of ReB_2 consists of alternating layers of hexagonal close-packed Re atoms and puckered hexagonal networks of B atoms. Apparently, the uncompressibility of ReB_2 along the *c*-axis is caused by the orientation of the Re–B bonds. However, the superhard characteristics of ReB_2 has been recently put into doubt [184], indicating that new studies are needed to better known the high-pressure properties of ReB_2. In other diborides, like AlB_2, TiB_2, VB_2, and ZrB_2, no phase transition has been observed up to 40–50 GPa [185–187]. Bulk moduli of 237 GPa, 322 GPa, and 317 GPa were found in TiB_2, VB_2, and ZrB_2, respectively; while that of AlB_2 is 170 GPa and its compressibility is moderately anisotropic, consistent with the anisotropic bonding properties in this material.

To conclude this section, we would like to comment the interesting case of framework structures of AX_2 compounds under pressure. CO_2 is well known by forming strongly-bound molecular phases at low pressures. At high pressures and temperatures the double C=O bonds are replaced by singly-bounded polymerized CO_4 groups (phase V) that form crystalline [188] and amorphous [189] framework structures analogous to SiO_2 and GeO_2. In fact, CO_2-V is likely a superhard material with the compressibility being similar to cubic-BN [188]. Zeolites are framework structures based on SiO_2 whose pressure dependence with different pressure media is still poorly understood. It is known that some zeolites undergo a phase transition to amorphous phases on increasing pressure [190]; however, a pressure-induced phase transition to a different zeolite crystalline structure still has not been reported.

2.5 ABX_2 compounds ABX_2 compounds can be seen as A_2X_2 compounds and consequently are related to AX compounds. Therefore, many structures of the ABX_2 compounds are superstructures of those present in the AX compounds. Among ABX_2 compounds the most studied are those of the chalcopyrite ($CuFeS_2$) family whose structure ($I\bar{4}2d$) is a zincblende structure doubled along the *c*-axis. These compounds have received considerable attention because many of them (like $CuInSe_2$ and $CuGaSe_2$) show promising electrical and optical properties for solar cell devices. The high-pressure behavior of the chalcopyrites has been extensively studied during the 90's [191–193]. Because these compounds are isoelectronic with the

zincblende II–VI semiconductors, they are expected to have a similar high-pressure structural sequence. Indeed a chalcopyrite to rocksalt transition is found at relative low pressures in $AgGaX_2$ (X = S, Se, and Te) [192], $CuAlS_2$, $CuGaS_2$, $CuInS_2$, $AgInSe_2$ and many other compounds [194], being the rocksalt structure the stable phase at ambient conditions in others like $AgSbTe_2$. In some compounds the transition is direct and in others it occurs through a disorder zincblende ($P\bar{4}$) or a α-$NaFeO_2$ structure (C2/m). The analogy between the chalcopyrite and the zincblende-structured binary compounds does not finish here. A second phase transition from the rocksalt structure to an orthorhombic Cmcm structure has been recently found in $CuGaTe_2$ and $CuInTe_2$. This structure is analogous to the post-rocksalt structure found in zincblende-structured CdTe and ZnTe [59]. Also similar to rocksalt-structured binary compounds, $AgSbTe_2$ has been found to undergo a transition from the rocksalt towards the CsCl phase [195]. Even though the systematic of phase transitions induced by pressure in chalcopyrites seems to be well established, in the lasts years there was a rebirth of the high-pressure studies on these compounds. These studies have been triggered by the fact that a chalcopyrite structure is predicted for the potential superhard boron-carbonitride (BC_2N) [196]. The new studies are focused not only in the nitrides but also in compounds like $CdGeP_2$ [197] and $CuFeS_2$ [198]. Static and dynamic structural properties of $CuFeS_2$ under high pressure have been investigated by X-ray diffraction and ^{57}Fe nuclear resonant inelastic scattering. These studies found evidence that a pressure-induced amorphization, accompanied of a metal–insulator transition, occurs at about 6.3 GPa. In spite of being the chalcopyrites a long-studied subject, much remains to be done in this field and that in the nearest future one may expect new interesting results.

Finally, other ABX_2 compounds related to chalcopyrites, whose pressure dependence is receiving attention in the last years, are the compounds crystallizing in the delafossite structure. Delafossite is the mineral $CuFeO_2$ whose structure is $R\bar{3}m$ and is the general name of ABX_2 compounds crystallizing in this structure like $CuAlO_2$, $CuGaO_2$, $CuScO_2$, $CuYO_2$ $AgAlO_2$, $AgGaO_2$, $AgInO_2$, and $AgScO_2$ among others. Some of them have been proposed for transparent conductive oxides for solar cells and flat panel displays. Recently, a phase transition to a still unresolved structure has been observed in $CuGaO_2$ and $CuAlO_2$ near 26 GPa and 34 GPa, respectively [199–201]. Similarly, two phase transitions to still unresolved structures have been found in $CuScO_2$ between 13 GPa and 18 GPa [202]. New and exciting high pressure results will help us to understand the special character of Cu and Ag in these compounds.

2.6 A_2X_3 compounds Sesquioxides (A_2O_3) are very important materials since they play a vital role in the processing of ceramics as additives, grain growth inhibitors, and phase stabilizers. They have also potential applications in nuclear engineering and as host optical materials for rare-earth phosphors. Besides, sesquioxides with corundum-like ($R\bar{3}m$) structure, like corundum (α-Al_2O_3), hematite (α-Fe_2O_3), and eskolaite (α-Cr_2O_3), are relevant to Earth Sciences because they are mantle minerals. Furthermore, the high-pressure behavior of corundum α-Al_2O_3 is of particular interest to high-pressure research owing to the common use of the ruby fluorescence scale to determine pressure in experiments using the DAC.

The corundum structure is also common to karelianite (V_2O_3) as well as Ti_2O_3, Ga_2O_3, and In_2O_3 and no pressure-induced phase transition is know in Al_2O_3 up to 100 GPa at RT. However, a phase transformation has been reported to occur around 100 GPa at temperatures exceeding 1000 K [203, 204]. Full-profile Rietveld refinements show that the high-pressure phase has the Rh_2O_3(II) (Pbcn) structure, which is structurally related to corundum, but with the AlO_6 polyhedra highly distorted. This structure was previously observed in Rh_2O_3 [205] and is in good agreement with theoretical predictions [206, 207]. Another phase transition to the Pbnm-perovskite structure is theoretically predicted in Al_2O_3 above 200 GPa [208, 209]. Similarly to α-Al_2O_3, α-Fe_2O_3 at RT transforms to the Rh_2O_3(II) phase above 50 GPa [210]. However, in situ high-pressure experiments using a laser heated DAC reported that α-Fe_2O_3 transforms to a perovskite (Pnma) structure at 30 GPa and to a post-perovskite $CaIrO_3$ (Cmcm) structure above 50–60 GPa [211, 212]. A similar transformation to the post-perovskite Cmcm phase was also observed in Al_2O_3 above 130 GPa at high temperatures [213, 214]. Curiously enough, this structure has been recently found in bixbyite Mn_2O_3 above 27 GPa, which does not crystallize in the corundum structure but in the cubic Ia3 structure [215].

Raman spectroscopy and X-ray diffraction measurements have been performed for pure Cr_2O_3 to 61 GPa with and without laser heating [216]. A color change, a splitting of Raman modes, a relative increase of some Raman mode intensities, a selective broadening of some diffraction lines, and systematic shifts of some diffraction peaks were found between 15 GPa and 30 GPa. The Raman spectrum and diffraction changes were consistent with a phase transition to the monoclinic V_2O_3 (I2/a) structure, which has also been observed in pure and Cr-doped V_2O_3 systems, but the observed changes were not consistent with a phase transition to the orthorhombic structure Rh_2O_3(II) or perovskite type. Above 30 GPa and after laser heating another new phase was found. The high-temperature phase has an orthorhombic unit cell as predicted by first-principles calculations [217] and Rietveld refinement shows that this could be either the Rh_2O_3-II or the perovskite-type structure.

To clarify apparent controversies between different high-pressure studies on sesquioxides, recently Ga_2O_3, and In_2O_3 have been studied. These compounds have been widely surveyed in the past as attractive semiconductors with a wide band-gap. Especially, their most stable phases at ambient condition, monoclinic β-Ga_2O_3 (E_g = 4.9 eV) and cubic In_2O_3 (E_g = 3.7 eV). The corundum structure of

these compounds (e.g. α-Ga_2O_3) can be generally prepared from their stable phase by high-pressure and temperature synthesis around 4 GPa and 1000 °C [218]. Corundum-structured Ga_2O_3 and In_2O_3 have been recently studied by X-ray diffraction up to 108 GPa and 20 GPa, respectively [219]. Rh_2O_3(II) phases were confirmed as post corundum phases for both Ga_2O_3 and In_2O_3 at about 37 GPa and 7 GPa, respectively. Recently, a new α-Gd_2S_3-type phase has been observed in In_2O_3 above 40 GPa (see Fig. 4) which could be found in other sesquioxides and even in ABO_3 compounds and which could be important to Earth Sciences [220].

The high-pressure behavior of rare-earth sesquioxides has also been recently studied. They crystallize in either the hexagonal ($P\bar{3}m1$) structure (A-type), the monoclinic C2/m structure (B-type), or the cubic Ia3 (C-type). The density and cation coordination of these structures increase in the order C, B, A; therefore, C to B, C to A, and B to A phase transitions are expected under compression. Examples of these pressure-driven phase transitions occur from C to B in Yb_2O_3 [221], from C to A in Sm_2O_3 [222] and in Gd_2O_3 [223] and from B to A structures in Sm_2O_3 [224]. The phase transition from C to B and afterwards from B to A was found in Y_2O_3 [225]. It has been also found that the cationic distances in the three structures of the rare-earth sesquioxides are similar to those in the bcc, fcc and hcp structures of the rare-earth metals [226]. According to a recent study in In_2O_3, where the Al_2O_3 phases and the rare-earth sesquioxide phases have been analyzed, the density increases in the sequence C-type → corundum → Rh_2O_3(II) → B-type → A-type. No pressure-driven phase transitions beyond the B- and A-type phases in rare-earth sesquioxides are known up to date. Possible candidates are the post-perovskite phase found in Mn_2O_3 and the α-Gd_2S_3-type phase observed in In_2O_3. Furthermore, it remains to be seen whether the high-pressure phases of rare-earth sesquioxides show cationic distances bearing resemblance with those of the high-pressure phases of parent metals as in the A, B, and C phases. Future studies in sesquioxides and sesquisulfides will bring undoubtedly new exciting results on the high-pressure behavior of A_2X_3 corundum-type compounds. In fact, the pressure behavior of B_2O_3 is highly complex and there are a number of unsolved questions in condensed matter physics in spite of its fundamental importance to the dynamics of magmatic melts in the Earth's interior [227].

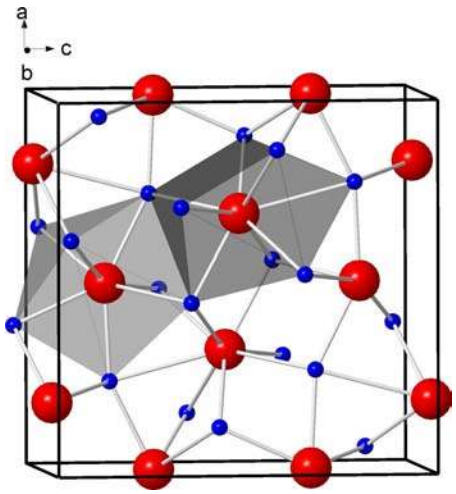

Figure 4 (online colour at: www.pss-b.com) Post-Rh_2O_3(II) phase (α-Gd_2S_3) in In_2O_3. Big red atoms are Gd and blue small atoms are S.

2.7 ABX_3 compounds ABX_3 compounds are related to A_2X_3 sesquioxides because the latter are a subgroup of the former where both A and B are the same cations. Consequently, many structures of the ABX_3 compounds are superstructures of those present in the sesquioxides. Besides, ABX_3 compounds are also related to ABC_2X_6 from whom ABX_3 compounds are a subgroup where A = B. ABX_3 compounds are relevant to Earth Sciences because many mantle minerals have this stoichiometry, like enstatite ($MgSiO_3$) which is one of the most important minerals that crystallizes in the orthorhombic pyroxene structure. Enstatite and ferrosilite ($FeSiO_3$) form a complete solid solution series that is found in igneous and metamorphic rocks coming from the Earth's lower mantle and meteorites and that crystallize either in the orthorhombic (orthopyroxene or protopyroxene) or in the monoclinic (clinopyroxene) symmetry. The pyroxene structure is also common to $ABSi_2O_6$ and $ABAl_2O_6$ compounds and is also found in the mineral wollastonite ($CaSiO_3$).

Under pressure $MgSiO_3$ and $MgGeO_3$ undergo the phase transition sequence: pyroxene → ilmenite → perovskite. However under certain conditions of pressure and temperature $MgSiO_3$ can also be transformed to the tetragonal garnet structure. Ilmenite is the mineral $FeTiO_3$ which has a trigonal structure ($R\bar{3}$) and is also the general name of the ABO_3 compounds crystallizing in this structure. Other compounds crystallizing in this structure are geikielite ($MgTiO_3$) and pyrophanite ($MnTiO_3$) that are minerals commonly mixed with ilmenite. The ilmenite structure is stable at ambient pressure in titanates and can be stabilized in germanates, like $MgGeO_3$, at moderate pressures, and in silicates, like $MgSiO_3$, at rather high pressures and temperatures (21–25 GPa and 1100 °C) [228]. The ilmenite structure is an ordered derivative of the corundum structure with two distinct cation sites, both in octahedral coordination. This structure is relatively incompressible, with a bulk modulus of 170 GPa ($FeTiO_3$). The compression is highly anisotropic and it is related to the compressibility of FeO_6 octahedra which are more compressible than the TiO_6 octahedra.

Perovskite is the name of the scarce mineral $CaTiO_3$ and is also the general name of ABO_3 compounds having the orthorhombic Pnma or Pbnm structure. This structure is very versatile and the compounds crystallizing in this structure have many useful technological applications such as ferroelectrics, multiferroics, magnetosresistors, catalysts,

sensors, thermopower and superconductors. Ilmenite-type $MgSiO_3$, also known as akimotoite, transforms to the perovskite structure around 25 GPa [229]. Perovskite-type $MgSiO_3$ is thought to be the most common mineral in the Earth mantle and it has been recently found that perovskite-type $MgSiO_3$ undergoes a phase transition above 125 GPa and 2500 K to the post-perovskite $CaIrO_3$ (Cmcm) structure (see Fig. 5) [230]. A huge scientific activity has resulted from the discovery of the post-perovskite phase whose aim is to explain the anomalous properties of the travel of seismic waves in the heterogeneous D″ layer of the Earth's lower mantle. Furthermore, the electrical conductivity of the post-perovskite phase and its electromagnetic coupling with Fe in the Earth's core has been proposed as the cause of the change of the Earth's rotation velocity which gives rise to the variation of the day length over decades [231–233].

Recent studies have reported the occurrence of pressure-driven phase transitions on the ilmenite family of compounds. Ilmenite-type $ZnGeO_3$ transformed into Pbnm perovskite at 30 GPa and 1300 K in a laser-heated DAC and after releasing the pressure, the $LiNbO_3$ phase (R3c) was recovered as a quenched product [234]. The perovskite structure of $ZnGeO_3$ was also obtained by recompression of the $LiNbO_3$ phase at RT under a lower pressure than the equilibrium phase boundary of the ilmenite-to-perovskite transition. In $FeTiO_3$ the phase transformation from ilmenite to perovskite was also observed using synchrotron-based X-ray diffraction and a large-volume press [25]. The perovskite phase is temperature quenchable at 20 GPa and converts into the $LiNbO_3$ phase at pressures below 15 GPa at RT. The $LiNbO_3$ phase of $FeTiO_3$ transforms into the ilmenite phase at 10 GPa and 673 K. However, the back-transformation from the ilmenite to the $LiNbO_3$ phase was not observed, thus strongly suggesting that the $LiNbO_3$ phase is not thermodynamically stable but rather a retrogressive phase formed from perovskite during decompression at RT. *Ab initio* calculations predict the transformation of the perovskite $FeTiO_3$ polymorph to a new high pressure polymorph with space group Cmcm at 44 GPa [235].

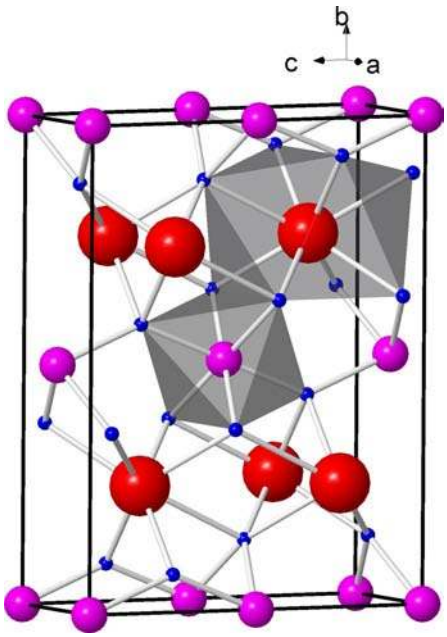

Figure 5 (online colour at: www.pss-b.com) Post-perovskite $CaIrO_3$ structure in $MgSiO_3$. Big red atoms are Mg, rose medium-sized atoms are Si, and small blue atoms are O.

Several groups are engaged today on the study of ilmenite-, perovskite-, and post-perovskite-structured compounds under compression and new interesting results are expected to come in the near future. For instance, a new post-perovskite oxide ($CaPtO_3$) has been recently synthesized at high pressures [236] and a perovskite-Pnma to monoclinic-$P2_1/m$ phase transition has been found in manganite $La_{0.5}Ca_{0.5}MnO_3$ above 15 GPa [237].

2.8 ABX_4 compounds ABX_4 materials are related to the AX_2 compounds since the latter are a subgroup of the former where both A and B are the same cations. Consequently, many structures of the ABX_4 compounds are superstructures of those present in the AX_2 compounds. The ABX_4 family contain many ternary compounds since cation A with valences +1, +2, +3, and + 4 can be accommodated with cation B with valences +7, +6, +5, and +4, respectively. The phase behaviour of ABX_4 scintillating materials is a challenging problem with many implications for other fields including technological applications and Earth and planetary sciences. In particular, they have been used during the last years as solid-state scintillators ($CaWO_4$ and $PbWO_4$), laser-host materials ($YLiF_4$), solid state lasers (YVO_4), and in other optoelectronic devices like eye-safe Raman laser ($SrWO_4$). Hazen and Finger already noted that the compressibility of ABO_4 compounds is related to the compressibility of their cation A polyhedra and that $A^{4+}B^{4+}O_4$ compounds were the less compressible of all ternary oxides ABO_4 [238]. Furthermore, the compressibility of zircon- and scheelite-structured compounds can be estimated if the A–X distance is known [239, 240]. Despite the first observation of high-pressure phase transitions in ABX_4 compounds dates back to the early 1960s, it is only in the recent years that a great progress has been done in the understanding of the pressure effects on the structural and electronic properties of these compounds. The phase transitions in these compounds were reviewed in the 1970's and 1980's [42, 43] and they have been recently reviewed on the light of recent experimental and theoretical advances [240]. Now the phase transitions in these compounds and those in AX_2 compounds can be understood on the light of the Fukunaga and Yamaoka's and of the Bastide's diagrams [42, 43].

Depero et al. have noted that a number of crystal structures in ABX_4 compounds, consist of BX_4 tetrahedra and AX_8 eight-coordinated polyhedra, which can be seen as two interpenetrating tetrahedra, known as bidisphenoids or dodecahedra [241]. Among these structures some important mineral structures as scheelite or zircon are included

where A and B cations form two interpenetrating diamond structures in a tetragonally distorted fcc array [86]. In fact, a phase transition to a structure with cations forming a perfect fcc structure has been predicted in scheelites at high temperature [86]. Zircon is the mineral $ZrSiO_4$ and also the general name of the compounds crystallizing in the tetragonal $I4_1/amd$ phase, like many ABO_4 silicates, vanadates, phosphates, and arsenates ($HfSiO_4$, YVO_4, YPO_4, and $YAsO_4$). Scheelite is the mineral $CaWO_4$ and the general name of the compounds crystallizing in the tetragonal $I4_1/a$ phase, like other alkaline-earth tungstates ($SrWO_4$ and $BaWO_4$), $PbWO_4$, alkaline-earth molybdates, $PbMoO_4$, $CdMoO_4$, and a number of fluorites ($YLiF_4$, $LuLiF_4$, $CaZnF_4$). Zircon and scheelite structures are superstructures of the rutile structure common in AX_2 compounds and the following pressure-driven phase transitions sequence can be predicted on the light of recent advances [240]: $I4_1/amd$ (zircon) → $I4_1/a$ (scheelite) → I2/a (fergusonite) → $P2_1/n$ ($BaWO_4$-II-type) → orthorhombic phases ($BaMnF_4$-type, Cmca) → amorphous. It has been shown that the fergusonite and $BaWO_4$-II type structures are competitive in scheelite-type alkaline-earth tungstates, being the fergusonite phase more favourable than the $BaWO_4$-II phase in compounds with small ionic radii of cation A and the converse holds for compounds with larger ionic radii of cation A [242]. Furthermore, the scheelite to fergusonite phase transition observed in many tungstates, molybdates and vanadates has been found to be a second-order character phase transition [39, 40, 243]. The phase transitions to the orthorhombic phases still have to be confirmed experimentally in zircon and scheelite-type compounds. The $BaMnF_4$ (CmC2) phase has been recently found in fergusonite-type $LaNbO_4$ at high pressures [244] but the $BaMnF_4$ and Cmca structures still have to be confirmed in zircon- and scheelite-type compounds at high pressures. Also the amorphous phase has to be explored since the amorphisation of several tungstates and molybdates has been reported but the structural evolution of fergusonite-like compounds (niobates, tantalates, and $HgWO_4$) and of $BaMnF_4$ have not been studied under high enough pressures.

Wolframite (P2/c), fergusonite (I2/a or C2/c), and the $BaWO_4$-II type structure ($P2_1/n$) are monoclinic deformations of zircon and scheelite structures. The occurrence of the wolframite to scheelite or of the scheelite to wolframite pressure-driven phase transition has been a long discussion that has been solved with the most recent experiments in scheelite-type alkaline-earth tungstates [31–34] and in wolframite $ZnWO_4$ [245]. Neither the scheelite to wolframite nor the wolframite to scheelite transition are expected to occur at high pressure. The only case for the scheelite to wolframite transition seems to be that of $CdMoO_4$ [246] which is a compound in the borderline of the stability of both structures according to the Bastide's diagram (see Refs. [240, 247]).

Another structure related to scheelite, and that deserves more studies under high pressure, is that of pseudoscheelite (Pnma) which is an orthorhombic distortion of the scheelite structure where the A cation has near 12 coordination and the B cation has four-fold coordination. The high pressure phases of several pseudoscheelites have been studied but their symmetry is still unresolved [248–251]. A pseudoscheelite to scheelite pressure-driven phase transition was previously assumed but this transition is not expected on the light of the Bastide's diagram. Pseudoscheelite-related compounds that are receiving attention lately are the alkali hydrates (ABH_4 with A = Li, Na, K, Rb, Cs and B = B, Al) for their potential use in hydrogen storage. Many materials have been explored under pressure in the hope of finding ways to produce novel structures with high volumetric hydrogen contents. A recent review of the high-pressure behavior in these systems has been recently published [252]. Borohydrides crystallize in the cubic $Fm\bar{3}m$ structure except $LiBH_4$ that crystallizes in the orthorhombic pseudoscheelite structure. The phase transitions in $LiBH_4$ are also to other structures than in the heavier alkali borohydrides. In KBH_4 two phase transitions from the $Fm\bar{3}m$ phase to the tetragonal $P42_1c$ structure at 3.8 GPa and further to the orthorhombic Pnma structure at 6.8 GPa have been observed [253]. On the other hand, alanates ($MAlH_4$) tend to crystallize in the tetragonal scheelite structure except $LiAlH_4$ that crystallizes in the monoclinic $P2_1/c$. A phase transition in $LiAlH_4$ above 7 GPa to the monoclinic I2/b structure has been observed [254]. However, a phase transition from the tetragonal scheelite phase to the monoclinic $P2_1/c$ structure in $NaAlH_4$ has been observed above 14 GPa [253].

Finally, the berlinite family is one of the families of most studied ABO_4 compounds under pressure due to their isoelectronic similarity with quartz SiO_2 and its importance for both materials and Earth sciences. In fact, the berlinite structure is the same α-quartz structure with the cell doubled along the *c*-axis due to the substitution of Si by A and B atoms. Phase transitions in berlinites were reviewed in Refs. [255, 256]. Berlinite is the mineral $AlPO_4$ and the general name of the ABO_4 compounds crystallizing in the

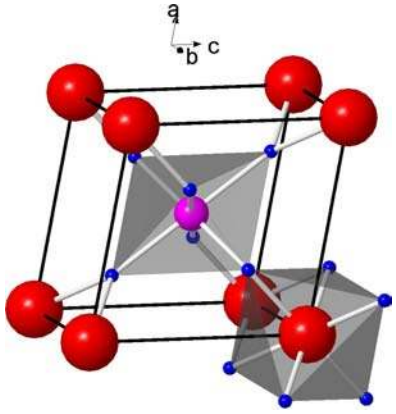

Figure 6 (online colour at: www.pss-b.com) Monoclinic structure found in $AlPO_4$ at high pressures with six-fold coordination for P. Big red atoms are Al, medium-sized atoms are P, and small blue atoms are O.

trigonal $P3_121$ structure, also known as low-quartz structure, like $GaPO_4$, $AlAsO_4$, and $GaAsO_4$. Similar compounds PBO_4, $AsBO_4$, and $InPS_4$ however crystallize in the high-cristobalite structure and undergo a pressure-induced phase transition to the berlinite structure at high pressures and temperatures [256–259]. Earlier was noted that berlinite-type $AlAsO_4$ undergo a phase transition to the rutile structure at 9 GPa and 900 °C [260]. Also $GaAsO_4$ undergoes a reversible phase transition around 8 GPa to a triclinic structure [261] and afterwards an irreversible phase transition to an amorphous rutile structure [262]. Recently, a new hexagonal high-pressure phase of $GaAsO_4$ has been reported [263, 264]. These results indicate that arsenates undergo phase transitions where an increase of As coordination from four to six is observed and that the observation of amorphisation is related to high kinetic energy barriers of the first-order phase transitions that cannot be overcome at RT. A similar increase of P coordination in $AlPO_4$ and $GaPO_4$ had not been observed under pressure [265, 266], and the pressure-induced amorphisation in $AlPO_4$ above 15 GPa showed a memory effect and was reversible unlike in other compounds [267–269]. A similar memory effect of amorphous phases is also observed in the collapsing of high crystobalites PBO_4 and $AsBO_4$ [270]. $FePO_4$ was found to transit from the berlinite structure to an orthorhombic Cmcm phase at 2.5 GPa and afterwards to an amorphous phase [271]. A big surprise has been the recent discovery of a monoclinic phase with P2/m symmetry and sixfold coordination for P in $AlPO_4$ above 47 GPa (see Fig. 6) [272]. The discovery of this new phase opens the way to obtain new materials with P in octahedral coordination and supports the two-step densification mechanism observed in isoelectronic SiO_2 [273, 274].

2.9 AB_2X_4 compounds The structure of AB_2X_4 compounds is related to those of AX and ABX_3 or B_2X_3 compounds. In fact, olivine (α-Mg_2SiO_4) with an orthorhombic Pbnm structure, and one of the most abundant minerals in the upper mantle, transforms to a modified spinel-type phase (β-Mg_2SiO_4) at 13.5 GPa, afterwards to a cubic spinel-type phase (γ-Mg_2SiO_4) above 18 GPa, and finally decomposes into perovskite-type $MgSiO_3$ and periclase MgO [275–278]. It was believed that the $\alpha-\beta$ and the $\beta-\gamma$ transitions in Mg_2SiO_4 are responsible for the seisimic discontinuities at 410 km and 660 km depths in the mantle, respectively. Therefore, the phase boundary between these diferent phases has been analysed in detail [279, 280] and the sound velocities of the different structures carefully measured [281].

Also important to Earth Science and technological applications is the behaviour under pressure of spinels like magnetite (Fe_3O_4 or more appropiately $Fe^{2+}Fe_2^{3+}O_4$). Magnetite crystallizes in the spinel structure ($Fd\bar{3}m$) typical of AB_2X_4 compounds where A and B cations are tetrahedrally and octahedrally coordinated to X anions, respectively. In this structure, partial inversion of the cations between the A and B sites is frequently observed. In particular, magnetite is an inverse spinel ($[Fe^{3+}]_A[Fe^{2+} + Fe^{3+}]_BO_4$) that suffers a modification of its population between the A and B sites with increasing pressure [282]. Pressure-induced phase transitions in oxide spinels were reviewed in the late 1960s [283] and it was found that while $A^{2+}B_2^{3+}O_4$ spinels tend to decomposition $A_2^{2+}B^{4+}O_4$ spinels tend to denser single phases or to mixtures of AO and ABO_3 phases. However, pressureinduced phase transitions in magnetite towards the orthorhombic $CaTiO_2$ (Bbmm) or $CaMn_2O_4$ (Pbcm) structures have been observed between 20 GPa and 60 GPa [284–287]. Similarly, hausmmanite (Mn_3O_4) has been found to transform to the marokite-type ($CaMn_2O_4$) structure at 14.2 GPa [288]. Other minerals characterized under high pressure are spinel ($MgAl_2O_4$) and gahnite ($ZnAl_2O_4$). These aluminates and $FeCr_2O_4$ were thought to be the less compressible of the naturally occuring oxide spinels [289] but it has been recently theoretically predicted that the bulk modulus of all oxide spinels is around 200 GPa [290, 291] and that the bulk modulus of spinels mainly depends on the anion [292]. $MgAl_2O_4$ decomposes into Al_2O_3 and MgO above 11 GPa [293, 294] in good agreement with theoretical calculations. In a similar way, MCr_2O_4 spinels with M = Mg, Mn, and Zn are theoretically predicted to decompose above 19 GPa, 23 GPa, and 34 GPa, respectively [295]. However, a recent study has shown that $ZnAl_2O_4$ is stable in the cubic spinel structure up to 43 GPa [296] and $MgAl_2O_4$ is found to transit above 25 GPa and 1773 K to the $CaFe_2O_4$ structure [293]. Similarly, spinel-type $CoFe_2O_4$ and $MgMn_2O_4$ undergo a phase transition above 30 GPa and 15 GPa to the orthorhombic $CaFe_2O_4$ and $CaMn_2O_4$ structures, respectively [297, 298].

The less studied spinels are those with selenium and sulfur instead of oxygen. Spinel $CdCr_2Se_4$ undergo a phase transition near 10 GPa to a phase with tetragonal symmetry [299], while spinels $CdIn_2S_4$, $MgIn_2S_4$ and $MnIn_2S_4$ undergo phase transitions to a double rocksalt phase of the $LiTiO_2$ type near 10 GPa [300–302]. On the contrary, a lot of interest is shown in ultrahard nitride spinels recently synthesized whose properties are being explored at high pressures [12, 303–305]. A review on the high-pressure chemistry of nitride-based materials has been recently published [14].

Finally, we want to mention that many AB_2X_4 compounds with X = S, Se, Te crystallize in the tetragonal defect-chalcopyrite ($I\bar{4}$) and defect-stannite ($I\bar{4}2m$) structures. These structures are superstructures of the chalcopyrite ABX_2 structure where there are stoichiometric vacancies that provide these compounds with non-linear susceptibility, optical activity, intense luminescence, and high photosensitivity. Furthermore, this family of semiconductors is also of interest as possible infrared-transmitting windows materials and they are also applied in various nonlinear optical devices and as gyrotropic media in narrow-band optical filters. Defect chalcopyrite $CdGa_2Se_4$ was observed to transit to the defect cubic NaCl-type structure ($Fm\bar{3}m$) above 21 GPa and on decreasing pressure it has been found to undergo a phase transition to a disordered zincblende structure [306]. A similar behavior has been

observed for defect-chalcopyrite $CdAl_2Se_4$ above 9 GPa [307], and for defect-stannite $ZnGa_2Se_4$ and defect-chalcopyrite $CdGa_2S_4$ above 16 GPa and 17 GPa, respectively [308]. Future high-pressure studies are needed to understand the systematic of phase transitions in olivines, spinels, defect-chalcopyrites and defect-stannites under pressure, especially at high temperatures, where new metastable phases at ambient conditions with interesting properties could be found.

3 Conclusions and future prospects In this work, we have given an overview of the study of pressure-driven phase transitions illustrated with many different examples. A discussion of the current state-of-the-art, recent developments, main directions of progress and areas with the greatest need for further developments is provided. The reviewed results are highly interdisciplinary incumbing fields that go from semiconductor and superconductor physics to mineral physics. Many examples have been covered along the article giving special attention to recent discoveries. A particular dramatic example is the experimental discovery and theoretical confirmation of a new phase of magnesium silicate ($MgSiO_3$) stable only at pressures above 100 GPa, which has had an inmediate and profound impact on studies of the Earth's deep mantle.

The results here reviewed show the huge progress done in the last decades on the knowledge of pressure-driven phase transitions. However, in many cases the mechanism of the transition is far from being understood and there is a lack of a systematic in the structural phase transitions for many families of compounds. Furthermore, in a recent review of oxide minerals Smyth et al. raised one question that has to be answered [35]: What is the role of cation–cation repulsion in the high-pressure behavior of minerals? In this respect, two old works and two recent works could give a clue to understand the role of cations in high-pressure phase transitions which could be crucial to the understanding of solid state chemistry. In the old works, the ionic model and the use of ionic radii are critically reviewed suggesting that the main role of pressure is to overcome cation–cation repulsion giving a preponderant role in crystal chemistry to non-bonded forces between cations [309, 310]. In the recent works, the ideas of these two old works are further developed showing that the role of oxygen in many oxides is similar to that of pressure [85] and that the pressure-induced phase transitions in AX, A_2X, AX_2, and ABX_n compounds (A and B being cations and X being anions) can be understood by generalizing the Zintl–Klemm concept and relating it with the stability of electronic distributions in group 14 compounds (group-IV semiconductors) according to the "8-N or octet" rule for electronic configurations [57].

As regards technical challenges, it is known that, before equilibrium is reached, phase transitions proceed as a function of time. Thus, investigating the kinetics of phase transition is also important and holding pressure constant while monitoring phase transformation is an overlooked issue that deserves more attention. Furthermore, many structural phase transitions are sensitive to stress conditions and the effect of non-hydrostatic stress on the conditions of phase equilibrium is still poorly understood. Besides, it has been recognized that in the study of phase transitions the presence of a second phase may affect the transition conditions of the former. Therefore, phase boundary may also be sensitive to the amount of minor or trace elements in the sample and this effect has to be more studied. Additionally, to ensure that the experimental data collected at micron or sub-micron scale are applicable to the bulk, we must also understand the effect of grain size, surface effect and the presence of nanometer-sized inclusions on phase transitions.

Finally, we must mention that two challenging projects in the high-pressure community concern single-crystal X-ray diffraction at Mbar pressures and combined studies of Brillouin and single-crystal X-ray diffraction. These techniques and other new generation of analytical methods, including the progress in high-pressure neutron diffraction, as well as future theoretical improvements will be fundamental to unroll the fascinating and challenging problem of pressure-induced phase transitions and they will have a deep impact in our understanding of condensed-matter physics.

Acknowledgements This study was supported by the Spanish government MEC under Grants No: MAT2006-02279, MAT2007-65990-C03-01, and CSD-2007-00045 and the Generalitat Valenciana (Projects GV2006/151 and GV2008/112). F. J. Manjón and D. Errandonea acknowledge financial support from "Vicerrectorado de Innovación y Desarrollo de la UPV" through project UPV20080020 and from the MEC of Spain through the "Ramón y Cajal" program, respectively. D. Errandonea is also indebted to the Fundación de las Artes y las Ciencias de Valencia for granting him the IDEA prize. The authors gratefully acknowledged A. Vegas for a critical reading of the manuscript.

References

[1] M. Eremets, High Pressure Experimental Methods (Oxford University Press, Oxford, 1996).
[2] R. J. Hemley, H. K. Mao, and V. V. Struzhkin, J. Synchrotron Radiat. **12**, 135 (2005).
[3] M. T. Yin and M. L. Cohen, Phys. Rev. Lett. **45**, 1004 (1980).
[4] M. C. Payne, M. P. Teter, D. C. Alan, T. A. Arias, and J. D. Joannopoulos, Rev. Mod. Phys. **64**, 1045 (1992).
[5] D. Errandonea, M. Somayazulu, D. Häusermann, and H. K. Mao, J. Phys.: Condens. Matter **15**, 7635 (2003).
[6] G. Trimarchi and A. Zunger, Phys. Rev. B **75**, 104113 (2007).
[7] T. Ogitsu, Nature Phys. **3**, 452 (2007).
[8] C. J. Pickard and R. J. Needs, Nature Phys. **3**, 473 (2007).
[9] A. R. Oganov and C. W. Glass, J. Phys.: Condens. Matter **20**, 064210 (2008).
[10] J. Behler, R. Martonak, D. Donadio, and M. Parrinello, Phys. Rev. Lett. **100**, 185501 (2008); Phys. Status Solidi B **245**, 2618 (2008).

[11] Y. Gogotsi, S. Welz, D. A. Ersoy, and M. J. McNallan, Nature **411**, 283 (2001) and references therein.
[12] P. F. McMillan, Nature Mater. **1**, 19 (2002).
[13] E. Gregoryanz, C. Sanloup, M. Somayazulu, J. Badro, G. Fiquet, H. K. Mao, and R. J. Hemley, Nature Mater. **3**, 294 (2004).
[14] E. Horvath-Bordon, R. Riedel, A. Zerr, P. F. McMillan, G. Auffermann, Y. Prots, W. Bronger, R. Kniep, and P. Kroll, Chem. Soc. Rev. **35**, 987 (2006).
[15] J. L. He, L. C. Guo, X. J. Guo, R. P. Liu, Y. J. Tian, H. T. Wang, and C. X. Gao, Appl. Phys. Lett. **88**, 101906 (2006).
[16] V. V. Brazhkin, High Press. Res. **27**, 333 (2007).
[17] J. C. Slater, Science **148**, 805 (1965).
[18] P. F. McMillan, Nature Mater. **4**, 715 (2005).
[19] P. W. Bridgman, The Physics of High Pressure (Bell, London, 1952).
[20] H. K. Mao and R. J. Hemley, Proc. Natl. Acad. Sci. **104**, 9114 (2007).
[21] W. B. Holzapfel and N. S. Isaacs (eds.), High Pressure Techniques in Chemistry and Physics (Oxford University Press, Oxford, 1997).
[22] R. J. Hemley and H. K. Mao (eds.), High Pressure Phenomena (IOS Press, Amsterdam, 2002).
[23] M. Yousuf, High Pressure Semiconductor Physics II, Semiconductor and Semimetals, Vol. 55 (Academic Press, London, 1998), p. 382.
[24] A. W. Lawson and T. Y. Tang, Rev. Sci. Instrum. **21**, 815 (1950).
[25] J. C. Jamieson, A. W. Lawson, and N. D. Nachtrieb, Rev. Sci. Instrum. **30**, 1016 (1959).
[26] C. E. Weir, E. R. Lippincott, A. Vanvalkenburg, J. Res. Natl. Bur. Stand. A **63**, 55 (1959).
[27] A. Ruoff, H. Xia, H. Luo, and Y. K. Vohra, Rev. Sci. Instrum. **61**, 3830 (1990).
[28] I. Goncharenko and P. Loubeyre, Nature **435**, 1206 (2005).
[29] J. M. Besson, G. Weil, G. Hamel, R. J. Nelmes, J. S. Loveday, and S. Hull, Phys. Rev. B **45**, 2613 (1992).
J. M. Besson, Ph. Pruzan, S. Klotz, G. Hamel, B. Silvi, R. J. Nelmes, J. S. Loveday, R. M. Wilson, and S. Hull, Phys. Rev. B **49**, 12540 (1994).
J. M. Besson and R. J. Nelmes, Physica B **213/214**, 31 (1995).
[30] A. Mujica, A. Rubio, A. Muñoz, and R. J. Needs, Rev. Mod. Phys. **75**, 863 (2003).
[31] D. Errandonea, J. Pellicer-Porres, F. J. Manjón, A. Segura, Ch. Ferrer-Roca, R. S. Kumar, O. Tschauner, P. Rodríguez-Hernández, J. López-Solano, S. Radescu, A. Mujica, A. Muñoz, and G. Aquilanti, Phys. Rev. B **72**, 174106 (2005).
[32] D. Errandonea, J. Pellicer-Porres, F. J. Manjón, A. Segura, Ch. Ferrer-Roca, R. S. Kumar, O. Tschauner, J. López-Solano, P. Rodríguez-Hernández, S. Radescu, A. Mujica, A. Muñoz, and G. Aquilanti, Phys. Rev. B **73**, 224103 (2006).
[33] F. J. Manjón, D. Errandonea, N. Garro, J. Pellicer-Porres, P. Rodríguez-Hernández, S. Radescu, J. López-Solano, A. Mujica, and A. Muñoz, Phys. Rev. B **74**, 144111 (2006).
[34] F. J. Manjón, D. Errandonea, N. Garro, J. Pellicer-Porres, J. López-Solano, P. Rodríguez-Hernández, S. Radescu, A. Mujica, and A. Muñoz, Phys. Rev. B **74**, 144112 (2006).
[35] J. R. Smyth, S. D. Jacobsen, and R. M. Hazen, Comparative Crystal Chemistry of Dense Oxide Minerals, in: Reviews in Mineralogy and Geochemistry, Vol. 41 (Mineralogical Society of America, 2000), p. 157.
[36] J. R. Smyth, S. D. Jacobsen, and R. M. Hazen, Comparative Crystal Chemistry of Orthosilicate Minerals, in: Reviews in Mineralogy and Geochemistry, Vol. 41 (Mineralogical Society of America, 2000), p. 187.
[37] L. Liu and W. A. Bassett, Elements, Oxides, Silicates: High-Pressure Phases with implications for the Earth's Interior (Oxford University Press, New York, 1986).
[38] R. A. Evarestov and V. P. Smirnov, Site Symmetry in Crystals: Theory and Applications (Springer, Berlin, 1993).
[39] D. Errandonea, Eur. Phys. Lett. **77**, 56001 (2007).
[40] D. Errandonea and F. J. Manjón, Mater. Res. Bull. **44**, DOI 10.1016/j.materresbull.2008.09.024 (2009).
[41] J. M. Besson, J. P. Itié, G. Weill, J. L. Mansot, and J. González, Phys. Rev. B **44**, 4214 (1991).
[42] O. Fukunaga and S. Yamaoka, Phys. Chem. Miner. **5**, 167 (1979).
[43] J. P. Bastide, J. Solid State Chem. **71**, 115 (1987) and references therein.
[44] A. W. Sleight, Acta Crystallogr. B **28**, 2899 (1972).
[45] J. W. Otto, J. K. Vassiliou, R. F. Porter, and A. L Ruoff, Phys. Rev. B **44**, 9223 (1991).
[46] D. B. McWhan, Science **176**, 751 (1972).
[47] C. W. F. T. Pistorius, Prog. Solid State Chem. **11**, 1 (1976).
[48] D. A. Young, Phase Diagrams of the Elements (University of California Press, Berkeley, 1991).
[49] U. Schwartz, Z. Kristallogr. **219**, 376 (2004).
[50] E. Yu Tonkov and E. G. Ponyatovsky, Phase Transformations of Elements under High Pressure (CRC Press, Boca Raton, 2005).
[51] M. I. McMahon and R. J. Nelmes, Chem. Soc. Rev. **35**, 943 (2006).
[52] H. L. Skriver, Phys. Rev. B **31**, 1909 (1985).
[53] D. Errandonea, R. Boehler, and M. Ross, Phys. Rev. B **65**, 012108 (2002).
[54] J. M. Perez-Mato, L. Elcoro, V. Petricek, H. Katzke, and P. Blaha, Phys. Rev. Lett. **99**, 025502 (2007).
[55] I. Loa, L. F. Lundegaard, M. I. McMahon, S. R. Evans, A. Bossak, and M. Krisch, Phys. Rev. Lett. **99**, 035501 (2007).
[56] O. Degtyareva, M. V. Magnitskaya, J. Kohanoff, G. Profeta, S. Scandolo, M. Hanfland, M. I. McMahon, and E. Gregoryanz, Phys. Rev. Lett. **99**, 155505 (2007).
[57] A. Vegas and V. G. Baonza, Acta Crystallogr. B **63**, 339 (2007).
[58] D. Santamaría-Pérez and A. Vegas, Acta Crystallogr. B **59**, 305 (2003).
[59] R. J. Nelmes and M. I. McMahon, High Pressure Semiconductor Physics I, Semiconductors and Semimetals, Vol. 54 (Academic Press, London, 1998), p. 146.
[60] E. A. Ekimov, V. A. Sidorov, E. D. Bauer, N. N. Mel'nik, N. J. Curro, J. D. Thomson, and S. M. Stishov, Nature **428**, 542 (2004).
[61] S. J. Duclos, Y. K. Vohra, and A. L. Ruoff, Phys. Rev. B **41**, 12021 (1990).
[62] K. Takemura, U. Schwartz, K. Syassen, M. Hanfland, N. E. Christensen, D. L. Novikov, and I. Loa, Phys. Rev. B **62**, R10603 (2000).

[63] S. Desgreniers, Y. K. Vohra, and A. L. Ruoff, Phys. Rev. B **39**, 10359 (1989).
[64] H. B. Cheong and K. J. Chang, Phys. Rev. B **44**, 4103 (1991).
[65] H. K. Mao, Y. Wu, J. F. Shu, J. Z. Hu, R. J. Hemley, and D. E. Cox, Solid State Commun. **74**, 1027 (1990).
[66] C. A. Vandenborgh, Y. K. Vohra, H. Xia, and A. L. Ruoff, Phys. Rev. B **41**, 7338 (1990).
[67] B. Sundqvist, Adv. Phys. **48**, 1 (1998).
[68] R. Moret, Acta Crystallogr. A **61**, 62 (2005).
[69] A. San-Miguel, Chem. Soc. Rev. **35**, 876 (2006).
[70] A. San-Miguel and P. Toulemonde, High Press. Res. **25**, 159 (2005).
[71] M. Beekman and G. S. Nolas, J. Mater. Chem. **18**, 842 (2008).
[72] R. F. W. Herrmann, K. Tanigaki, S. Kuroshima, and H. Suematsu, Chem. Phys. Lett. **283**, 29 (1998).
[73] S. Yamanaka, E. Enishi, H. Fukuoka, and M. Yasukawa, Inorg. Chem. **39**, 56 (2000).
[74] G. K. Ramachandran, P. F. McMillan, S. K. Deb, M. Somayazulu, J. Gryko, J. J. Dong, and O. F. Sankey, J. Phys.: Condens. Matter **12**, 4013 (2000).
[75] A. Jayaraman, Phys. Rev. **135**, A1056 (1964).
[76] B. Johansson and A. Rosengren, Phys. Rev. B **11**, 2836 (1975).
[77] D. Errandonea, R. Boehler, and M. Ross, Phys. Rev. Lett. **85**, 3444 (2000).
[78] N. C. Cunningham, W. Qiu, K. M. Hope, H. P. Liermann, and Y. K. Vohra, Phys. Rev. B **76**, 212101 (2007).
[79] D. Errandonea, R. Boehler, B. Schwager, and M. Mezouar, Phys. Rev. B **75**, 014103 (2007).
[80] J. Baer, H. Cynn, V. Iota, C. S. Yoo, and G. Shen, Phys. Rev. B **67**, 134115 (2003).
[81] N. C. Cunningham, N. Velisavljevic, and Y. K. Vohra, Phys. Rev. B **71**, 012108 (2005).
[82] B. Johansson and S. Li, J. Alloys Compd. **444/445**, 202 (2007) and references therein.
[83] J. R. Chelikowsky, Phys. Rev. B **34**, 5295 (1986).
[84] D. Santamaría-Pérez, A. Vegas, and F. Liebau, The Zinth–Klemm concept applied to cations in oxides II. The structures of silicates, in: Structure and Bonding, Vol. 118, (Springer, Berlin, 2005), p. 121.
[85] L. A. Martínez-Cruz, A. Ramos-Gallardo, and A. Vegas, J. Solid State Chem. **110**, 397 (1994).
[86] A. Vegas and M. Jansen, Acta Crystallogr. B **58**, 38 (2002).
[87] T. Huang and A. L. Ruoff, J. Appl. Phys. **54**, 5459 (1983).
[88] V. Ozolins and A. Zunger, Phys. Rev. Lett. **82**, 767 (1999).
[89] K. Kim, V. Ozolins, and A. Zunger, Phys. Rev. B **60**, R8449 (1999).
[90] A. Zunger, K. Kim, and V. Ozolins, Phys. Status Solidi B **223**, 369 (2001).
[91] J. López-Solano, A. Muñoz, and A. Mujica, Phys. Status Solidi B **244**, 274 (2007).
[92] V. V. Scchennikov and S. V. Ovsyannikov, Phys. Status Solidi B **244**, 437 (2007).
[93] M. Catti, Phys. Rev. Lett. **87**, 035504 (2001).
[94] J. Cai and N. Chen, J. Phys.: Condens. Matter **19**, 266207 (1999).
[95] H. G. Zimmer, H. Winzen, and K. Syassen, Phys. Rev. B **32**, 4066 (1985).
[96] S. T. Weir, Y. K Vohra, and A. L. Ruoff, Phys. Rev. B **33**, 4221 (1986).
[97] H. Luo, R. G. Greene, and A. L. Ruoff, Phys. Rev. B **49**, 15341 (1994).
[98] H. Luo, R. G. Greene, K. Ghandehari, T. Li, and A. L. Ruoff, Phys. Rev. B **50**, 16232 (1994).
[99] C. Y. Yeh, Z. W. Lu, S. Froyen, and A. Zunger, Phys. Rev. B **46**, 10086 (1992).
[100] T. Li, H. Luo, R. G. Greene, A. L. Ruoff, S. S. Trail, and F. J. Disalvo, Phys. Rev. Lett. **74**, 5232 (1995).
[101] Y. Li, Y. Ma, T. Cui, Y. Yan, and G. Zou, Appl. Phys. Lett. **92**, 101907 (2008).
[102] A. L. Ruoff, T. Li, A. C. Ho, H. Luo, R. G. Greene, C. Narayana, J. C. Molstad, S. S. Trail, F. J. Disalvo, and P. E. VanCamp, Phys. Rev. Lett. **81**, 2723 (1998).
[103] P. E. VanCamp, V. E. VanDoren, and J. L. Martins, Phys. Rev. B **55**, 775 (1997).
[104] R. M. Hazen and R. Jeanloz, Rev. Geophys. Space Phys. **22**, 37 (1984).
[105] H. K. Mao et al., Phys. Earth Planet. Inter. **96**, 135 (1996).
[106] R. Cohen and Z. Gong, Phys. Rev. B **50**, 12301 (1994).
[107] R. Boehler, M. Ross, and D. B. Boercker, Phys. Rev. Lett. **78**, 4589 (1997).
[108] J. M. Recio, M. Florez, E. Francisco, M. A. Blanco, and M. Pendas, High Press. Res. **22**, 443 (2002).
[109] T. E. Slykhouse and H. G. Drickamer, J. Phys. Chem. Solids **7**, 207 (1958).
[110] G. S. Nunes, P. B. Allen, and J. L. Martins, Phys. Rev. B **57**, 5098 (1998) and references therein.
[111] P. Pichet, H. K. Mao, and P. M. Bell, J. Geophys. Res. **93**, 15279 (1988).
[112] B. Amrani, T. Benmessabih, M. Tahiri, I. Chiboub, S. Hiadsi, and F. Hamdache, Physica B **381**, 179 (2006) and references therein.
[113] M. Catti, Phys. Rev. B **74**, 174105 (2006).
[114] O. Mishima, Nature **310**, 393 (1984).
[115] O. Mishima, Nature **384**, 546 (1996).
[116] H. E. Stanley, S. V. Buldyrev, M. Canpolat, O. Mishima, M. R. Sadr-Lahijany, A. Scala, and F. W. Starr, Phys. Chem. Chem. Phys. **2**, 1551 (2000).
[117] K. Umemoto, R. M. Wentzcovitz, S. Baroni, and S. de Gironcoli, Phys. Rev. Lett. **92**, 105502 (2004).
[118] S. Klotz, Th. Strässle, R. J. Nelmes, J. S. Loveday, G. Hamel, G. Rousse, B. Canny, J. C. Chervin, and A. M. Saitta, Phys. Rev. Lett. **94**, 025506 (2005).
[119] A. Lazicki, C.-S. Yoo, W. J. Evans, and W. E. Pickett, Phys. Rev. B **73**, 184120 (2006).
[120] K. Kunc, I. Loa, and K. Syassen, Phys. Rev. B **77**, 094110 (2008).
[121] A. Grzechnik, A. Vegas, K. Syassen, I. Loa, M. Hanfland, and M. Jansen, J. Solid State Chem. **154**, 603 (2000).
[122] A. Vegas, A. Grzechnik, K. Syassen, I. Loa, M. Hanfland, and M. Jansen, Acta Crystallogr. B **57**, 151 (2001).
[123] A. Vegas, A. Grzechnik, M. Hanfland, C. Muhle, and K. Syassen, Solid State Sci. **4**, 1077 (2002).
[124] P. Demontis, R. LeSar, and M. L. Klein, Phys. Rev. Lett. **60**, 2284 (1988).
[125] P. Demontis, M. L. Klein, and R. LeSar, Phys. Rev. B **40**, 2716 (1989).

[126] K. Kunc, I. Loa, A. Grzechnik, and K. Syassen, Phys. Status Solidi B **242**, 1857 (2005).
[127] Z. Cancarevic, J. C. Schon, and M. Jansen, Phys. Rev. B **73**, 224114 (2006).
[128] A. Werner and H. D. Hochheimer, Phys. Rev. B **25**, 5929 (1982).
[129] D. Errandonea, D. Santamaría-Pérez, A. Vegas, J. Nuss, M. Jansen, P. Rodríguez-Hernández, and A. Muñoz, Phys. Rev. B **77**, 094113 (2008).
[130] J. M. Léger and J. Haines, Eur. J. Solid State Inorg. Chem. **34**, 785 (1997).
[131] P. J. Heaney, Rev. Mineral. **29**, 1 (1994).
[132] R. J. Hemley, C. T. Prewitt, and K. J. Kingma, Rev. Mineral. **29**, 41 (1994).
[133] K. J. Kingma, R. E. Cohen, R. J. Hemley, and H. K. Mao, Nature **374**, 243 (1995).
[134] D. Andrault, G. Fiquet, F. Guyot, and M. Hanfland, Science **282**, 720 (1998).
[135] L. S. Dubrovinsky, S. K. Saxena, P. Lazor, R. Ahuja, O. Eriksson, J. M. Wills, and B. Johansson, Nature **388**, 362 (1997).
[136] J. Haines, J. M. Léger, F. Gorelli, and M. Hanfland, Phys. Rev. Lett. **87**, 155503 (2001).
[137] R. M. Hazen and L. W. Finger, J. Phys. Chem. Solids **42**, 143 (1981).
[138] Y. Kudoh and H. Takeda, Physica B & C **139**, 333 (1986).
[139] M. Magnani, J. Geophys. Res. **74**, 4317 (1969).
[140] J. K. Kingma, H. K. Mao, and R. J. Hemley, High Press. Res. **14**, 363 (1996).
[141] S. Ono, T. Tsuchiya, K. Hirose, and Y. Ohishi, Phys. Rev. B **68**, 134108 (2003).
[142] J. Haines and J. M. Léger, Phys. Rev. B **55**, 11144 (1997).
[143] S. Ono, E. Ito, T. Katsura, A. Yoneda, J. M. Walter, S. Urakawa, W. Utsumi, and K. Funakoshi, Phys. Chem. Miner. **27**, 618 (2000).
[144] S. Ono, K. Hirose, M. Murakami, and M. Isshiki, Earth Planet. Sci. Lett. **197**, 187 (2002).
[145] J. E. Lowther, J. K. Dewhurst, J. M. Léger, and J. Haines, Phys. Rev. B **60**, 14485 (1999).
[146] S. J. Duclos, Y. K. Vohra, A. L. Ruoff, A. Jayaraman, and G. P. Espinosa, Phys. Rev. B **38**, 7755 (1988).
[147] L. Gerward and J. S. Olsen, J. Appl. Cryst. **30**, 259 (1997).
[148] W. Luo, S. F. Yang, Z. C. Wang, Y. Wang, R. Ahuja, B. Johansson, J. Liu, and T. Zou, Solid State Commun. **133**, 49 (2005).
[149] T. Sasaki, J. Phys.: Condens. Matter **14**, 10557 (2002).
[150] H. Arashi, T. Yagi, S. Akimoto, and Y. Kudoh, Phys. Rev. B **41**, 4309 (1990).
[151] L. S. Dubrovinsky, N. A. Dubrovinskaia, V. Swamy, J. Muscat, N. M. Harrison, R. Ahuja, B. Holm, and B. Johansson, Nature **410**, 653 (2001).
[152] M. Mattesini, J. S. de Almeida, L. Dubrovinsky, N. A. Dubrovinskaia, B. Johansson, and R. Ahuja, Phys. Rev. B **70**, 212101 (2004).
[153] Y. C. Liang, B. Zhang, and J. Z. Zhao, Phys. Rev. B **77**, 094126 (2008).
[154] V. P. Prakapenka, G. Y. Shen, L. S. Dubrovinsky, M. L. Rivers, and S. R. Sutton, J. Phys. Chem. Solids **65**, 1537 (2004).
[155] T. Sato, N. Funamori, T. Yagi, and N. Miyajima, Phys. Rev. B **72**, 092101 (2005).
[156] J. M. Léger, J. Haines, and A. Atouf, J. Appl. Crystallogr. **28**, 416 (1995).
[157] J. M. Léger, J. Haines, and A. Atouf, J. Phys. Chem. Solids **57**, 7 (1996).
[158] N. V. Chandra Shekar, P. Ch. Sahu, M. Yousuf, K. Govinda Rajan, and M. Rajagopalan, Solid State Commun. **111**, 529 (1999).
[159] H. Sugiura, I. Marchuk, V. Paul-Boncour, A. Percheron-Guégan, T. Kitazawa, and S. M. Filipek, J. Alloys Compd. **356/357**, 32 (2003).
[160] H. Sugiura, V. Paul-Boncour, A. Percheron-Guégan, I. Marchuk, T. Hirata, S. M. Filipek, and M. Dogorova, J. Alloys Compd. **367**, 230 (2004).
[161] A. Lindbaum, S. Heathman, T. Le Bihan, and P. Rogl, J. Alloys Compd. **298**, 177 (2000).
[162] B. K. Godwal, V. Vijaykumar, S. K. Sikka, and R. Chidambaram, J. Phys. F, Met. Phys. **16**, 1415 (1986).
[163] J. Feng, N. W. Ashcroft, and R. Hoffmann, Phys. Rev. Lett. **98**, 247002 (2007).
[164] J. R. Kessler, E. Monberg, and M. Nicol, J. Chem. Phys. **60**, 5057 (1974).
[165] G. A. Kourouklis and E. Anastassakis, Phys. Rev. B **34**, 1233 (1986).
[166] T. Hongo, K. G. Nakamura, T. Atou, M. Kikuchi, K. Yubuta, S. Itoh, K. Kusaba, K. Fukuoka, and K. Kondo, Phys. Rev. B **76**, 104114 (2007).
[167] M. Idiri, T. Le Bihan, S. Heathman, and J. Rebizant, Phys. Rev. B **70**, 014113 (2004).
[168] F. Merlo, A. Palenzon, and M. Pan, J. Alloys Compd. **348**, 173 (2003).
[169] J. M. Léger, J. Haines, and C. Danneels, J. Phys. Chem. Solids **59**, 1199 (1998).
[170] T. Moriwaki, Y. Akahama, H. Kawamura, S. Nakano, and K. Takemura, J. Phys. Soc. Jpn. **75**, 074603 (2006).
[171] K. Kinoshita, M. Nishimura, Y. Akahama, and H. Kawamura, Solid State Commun. **141**, 69 (2007).
[172] P. E. Kalita, A. L. Cornelius, K. E. Lipinska-Kalita, C. L. Gobin, and H. P. Liermann, J. Phys. Chem. Solids **69**, 2240 (2008).
[173] D. Errandonea, Y. Meng, M. Somayazulu, and D. Häusermann, Physica B **355**, 116 (2005).
[174] J. H. Weaver and D. J. Peterman, Phys. Rev. B **23**, 1692 (1981).
[175] M. Pozzo and D. Alfè, Phys. Rev. B **77**, 104103 (2008).
[176] D. Errandonea, Y. Meng, D. Häusermann, and T. Uchida, J. Phys.: Condens. Matter **15**, 1277 (2003).
[177] P. Bordet, M. Mezouar, M. Nunez-Regueiro, M. Monteverde, M. D. Nunez-Regueiro, N. Rogado, K. A. Regan, M. A. Hayward, T. He, S. M. Loureiro, and R. J. Cava, Phys. Rev. B **64**, 172502 (2001).
[178] B. K. Godwal, P. Modak, A. K. Verma, D. M. Gaitonde, and R. S. Rao, Curr. Sci. **85**, 1050 (2003).
[179] D. Errandonea, J. Phys. Chem. Solids **67**, 2017 (2006).
[180] O. Tschauner, D. Errandonea, and G. Serghiou, Physica B **371**, 88 (2006).
[181] J. Nagamatsu, N. Nakagawa, T. Muranaka, Y. Zenitani, and J. A. Kimitsu, Nature **410**, 63 (2001).
[182] G. M. Amulele and M. H. Manghnani, J. Appl. Phys. **97**, 023506 (2005).

[183] H. Y. Chung, M. B. Weinberger, J. B. Levine, A. Kavner, J. M. Yang, S. H. Tolbert, and R. B. Kaner, Science **316**, 436 (2007).
[184] N. Dubrovinskaia, L. Dubrovinsky, and V. L. Solozhenko, Science **318**, 5856 (2007).
[185] R. G. Munroe, J. Res. Natl. Inst. Stand. Technol. **105**, 709 (2000).
[186] A. S. Pereira, C. A. Perottoni, J. A. H. da Jornada, J. M. Léger, and J. Haines, J. Phys.: Condens. Matter **14**, 10615 (2002).
[187] I. Loa, K. Kunc, K. Syassen, and P. Bouvier, Phys. Rev. B **66**, 134101 (2002).
[188] C. S. Yoo, H. Cynn, F. Gygi, G. Galli, V. Iota, M. Nicol, S. Carlson, D. Häussermann, and C. Mailhiot, Phys. Rev. Lett. **83**, 5527 (1999).
[189] M. Santoro, F. A. Gorelli, R. Bini, G. Ruocco, S. Scandolo, and W. A. Crichton, Nature **441**, 857 (2006).
[190] G. N. Greaves, F. Meneau, F. Kargl, D. Ward, P. Holliman, and F. Albergamo, J. Phys.: Condens. Matter **19**, 415102 (2007).
[191] J. González, M. Quintero, and C. Rincón, Phys. Rev. B **45**, 7022 (1992).
[192] Y. Mori, S.-I. Iwamoto, K.-I. Takarabe, S. Minomura, and A. L. Ruoff, Phys. Status Solidi B **211**, 469 (1999).
[193] R. S. Kumar, A. Sekar, N. V. Jaya, S. Natarajan, and S. Chichibu, J. Alloys Compd. **312**, 4 (2000).
[194] V. V. Ursaki, I. I. Burlakov, I. M. Tiginyanu, Y. S. Raptis, E. Anastassakis, and A. Anedda, Phys. Rev. B **59**, 257 (1999).
[195] R. S. Kumar, A. L. Cornelius, E. Kim, Y. Shen, S. Yoneda, C. F. Chen, and M. F. Nicol, Phys. Rev. B **72**, 060101 (2005).
[196] J. Sun, X. F. Zhou, G. R. Qian, J. Chen, Y. X. Fan, H. T. Wang, X. J. Guo, J. L. He, Z. Y. Liu, and Y. J. Tian, Appl. Phys. Lett. **89**, 151911 (2006).
[197] I. H. Choi and P. Y. Yu, Phys. Status Solidi B **241**, 3138 (2004).
[198] H. Kobayashi, J. Umemura, Y. Kazekami, N. Sakai, D. Alfè, Y. Ohishi, and Y. Yoda, Phys. Rev. B **76**, 134108 (2007).
[199] J. Pellicer-Porres, A. Segura, C. Ferrer-Roca, D. Martinez-Garcia, J. A. Sans, E. Martinez, J. P. Itie, A. Polian, F. Baudelet, A. Muñoz, P. Rodríguez-Hernández, and P. Munsch, Phys. Rev. B **69**, 024109 (2004).
[200] J. Pellicer-Porres, A. Segura, E. Martinez, A. M. Saitta, A. Polian, J. C. Chervin, and B. Canny, Phys. Rev. B **72**, 064301 (2005).
[201] J. Pellicer-Porres, D. Martinez-Garcia, A. Segura, P. Rodriguez-Hernandez, A. Muñoz, J. C. Chervin, N. Garro, and D. Kim, Phys. Rev. B **74**, 184301 (2006).
[202] S. Gilliland, J. Pellicer-Porres, A. Segura, A. Muñoz, P. Rodriguez-Hernandez, D. Kim, M. S. Lee, and T. Y. Kim, Phys. Status Solidi B **244**, 309 (2007).
[203] N. Funamori and R. Jeanloz, Science **278**, 1109 (1997).
[204] J. F. Lin, O. Degtyareva, C. T. Prewitt, P. Dera, N. Sata, E. Gregoryanz, H. K. Mao, and R. J. Hemley, Nature Mater. **3**, 389 (2004).
[205] R. D. Shannon and C. T. Prewitt, J. Solid State Chem. **2**, 134 (1970).
[206] K. T. Thomson, R. M. Wentzcovitch, and M. S. T. Bukowinski, Science **274**, 1880 (1996).
[207] J. Tsuchiya, T. Tsuchiya, and R. M. Wentzcovitch, Phys. Rev. B **72**, 020103 (2005).
[208] K. T. Thomson, R. M. Wentzcovitch, and M. S. T. Bukowinski, Science **274**, 1880 (1996).
[209] W. Duan, R. M. Wentzcovitch, and K. T. Thomson, Phys. Rev. B **57**, 10363 (1998).
[210] M. P. Pasternak, G. Kh. Rozenberg, G. Yu. Machavariani, O. Naaman, R. D. Taylor, and R. Jeanloz, Phys. Rev. Lett. **82**, 4663 (1999).
[211] S. Ono, T. Kikegawa, and Y. Ohishi, J. Phys. Chem. Solids **65**, 1527 (2004).
[212] S. Ono, K. Funakoshi, Y. Ohishi, and E. Takahashi, J. Phys.: Condens. Matter **17**, 269 (2005).
[213] A. R. Oganov and S. Ono, Proc. Natl. Acad. Sci. **102**, 10828 (2005).
[214] S. Ono, A. R. Oganov, T. Koyama, and H. Shimizu, Earth Planet. Sci. Lett. **246**, 326 (2006).
[215] J. Santillán, S.-H. Shim, G. Shen, and V. B. Prakapenka, Geophys. Res. Lett. **33**, L15307 (2006).
[216] S. H. Shim, T. S. Duffy, R. Jeanloz, C. S. Yoo, and V. Iota, Phys. Rev. B **69**, 144107 (2004).
[217] W. Duan, G. Paiva, R. M. Wentzcovitch, and A. Fazzio, Phys. Rev. Lett. **81**, 3267 (1998).
[218] H. Mizoguchi and P. M. Woodward, Chem. Mater. **16**, 5233 (2004).
[219] H. Yusa, T. Tsuchiya, N. Sata, and Y. Ohishi, Phys. Rev. B **77**, 064107 (2008).
[220] H. Yusa, T. Tsuchiya, J. Tsuchiya, N. Sata, and Y. Ohishi, Phys. Rev. B **78**, 092107 (2008).
[221] Y. Hinuma, Y. Meng, K. Kang, and G. Ceder, Chem. Mater. **19**, 1790 (2007).
[222] Q. Guo, Y. Zhao, C. Jiang, W. L. Mao, and Z. Wang, Solid State Commun. **145**, 250 (2008).
[223] H. Y. Chen, C. Y. He, C. X. Gao, J. H. Zhang, S. Y. Gao, H. L. Lu, Y. G. Nie, D. M. Li, S. H. Kan, and G. T. Zou, Chin. Phys. Lett. **24**, 158 (2007).
[224] T. Hongo, K. Kondo, K. G. Nakamura, and T. Atou, J. Mater. Sci. **42**, 2582 (2007).
[225] E. Husson, C. Proust, P. Gillet, and J. P. Itié, Mater. Res. Bull. **34**, 2085 (1999).
[226] A. Vegas and R. Isea, Acta Crystallogr. B **54**, 732 (1998).
[227] S. K. Lee, K. Mibe, Y. Fei, G. D. Cody, and B. O. Mysen, Phys. Rev. Lett. **94**, 165507 (2005).
[228] E. Ito and Y. Matsui, Phys. Chem. Miner. **4**, 265 (1979).
[229] K. Hirose, T. Komabayashi, M. Murakami, and K. Funakoshi, Geophys. Res. Lett. **28**, 4351 (2001).
[230] M. Murakami, K. Hirose, K. Kawamura, N. Sata, and Y. Ohishi, Science **304**, 855 (2004).
[231] D. Cyranoski, Nature **440**, 1108 (2006).
[232] T. S. Duffy, Nature **451**, 269 (2008).
[233] K. Ohta, S. Onoda, K. Hirose, R. Sinmyo, K. Shimizu, N. Sata, Y. Ohishi, and A. Yasuhara, Science **320**, 89 (2008).
[234] Y. Hitoshi, A. Masaki, N. Sata, K. Hiroshi, Y. Ryo, and Y. Ohishi, Phys. Chem. Miner. **33**, 217 (2006).
[235] L. C. Ming, Y. H. Kim, T. Uchida, Y. Wang, and M. Rivers, Am. Mineral. **91**, 120 (2006).
[236] K. Ohgushi, Y. Matsushita, N. Miyajima, Y. Katsuya, M. Tanaka, F. Izumi, H. Gotou, Y. Ueda, and T. Yagi, Phys. Chem. Miner. **35**, 189 (2008).

[237] D. P. Kozlenko, L. S. Dubrovinsky, I. N. Goncharenko, B. N. Savenko, V. I. Voronin, E. A. Kiselev, and N. V. Proskurnina, Phys. Rev. B **75**, 104408 (2007).
[238] R. M. Hazen, L. W. Finger, and J. W. E. Mariathasan, J. Phys. Chem. Solids **46**, 253 (1985).
[239] D. Errandonea, F. J. Manjón, M. Somayazulu, and D. Häusermann, J. Solid State Chem. **177**, 1087 (2004).
[240] D. Errandonea and F. J. Manjón, Prog. Mater. Sci. **53**, 711 (2008).
[241] L. E. Depero and L. Sangaletti, J. Solid State Chem. **129**, 82 (1997).
[242] J. López-Solano, P. Rodríguez-Hernández, S. Radescu, A. Mujica, A. Muñoz, D. Errandonea, F. J. Manjón, N. Garro, J. Pellicer-Porres, A. Segura, Ch. Ferrer-Roca, R. S. Kumar, O. Tschauner, and G. Aquilanti, Phys. Status Solidi B **244**, 325 (2007).
[243] D. Errandonea, R. S. Kumar, X. Ma, and C. Y. Tu, J. Solid State Chem. **181**, 355 (2008).
[244] Y. A. Titov, A. M. Sych, A. N. Sokolov, V. Y. Markiv, N. M. Belyavina, and A. A. Kapshuk, High Press. Res. **21**, 175 (2001).
[245] D. Errandonea, F. J. Manjón, N. Garro, P. Rodríguez-Hernández, S. Radescu, A. Mujica, A. Muñoz, and C. Y. Tu, Phys. Rev. B **78**, 054116 (2008).
[246] A. Jayaraman, S. Y. Wang, and S. K. Sharma, Phys. Rev. B **52**, 9886 (1995).
[247] F. J. Manjón, D. Errandonea, J. López-Solano, P. Rodríguez-Hernández, S. Radescu, A. Mujica, A. Muñoz, N. Garro, J. Pellicer-Porres, A. Segura, Ch. Ferrer-Roca, R. S. Kumar, O. Tschauner, and G. Aquilanti, Phys. Status Solidi B **244**, 295 (2007).
[248] A. Jayaraman, G. A. Kourouklis, and L. G. Van Uitert, Phys. Rev. B **36**, 8547 (1987).
[249] A. Jayaraman, G. A. Kourouklis, L. G. Van Uitert, W. G. Grodkiewicz, and R. G. Maines, Physica A **156**, 325 (1989).
[250] N. Chandrabas, D. Victor, S. Muthu, A. K. Sood, H. L. Bhat, and A. Jayaraman, J. Phys. Chem. Solids **53**, 959 (1992).
[251] L. C. Ming, A. Jayaraman, S. R. Shieh, and Y. H. Kim, Phys. Rev. B **51**, 12100 (1995).
[252] B. Sundqvist, O. Anderson, and A. V. Talyzin, J. Phys.: Condens. Matter **19**, 425201 (2007).
[253] R. S. Kumar, E. Kim, O. Tschauner, and A. L. Cornelius, Phys. Rev. B **75**, 174110 (2007).
[254] M. P. Pitt, D. Blanchard, B. C. Hauback, H. Fellvag, and W. G. Marshall, Phys. Rev. B **72**, 214113 (2005).
[255] A. Polian, J. P. Itié, M. Grimsditch, J. Badro, and E. Philippot, Eur. J. Solid State Inorg. Chem. **34**, 669 (1997).
[256] J. Haines and O. Cambon, Z. Kristallogr. **219**, 314 (2004).
[257] F. Dachille and L. S. D. Glasser, Acta Crystallogr. **12**, 820 (1959).
[258] J. M. Leger, J. Haines, L. S. de Oliveira, C. Chateau, A. Le Sauze, R. Marchand, and S. Hull, J. Phys. Chem. Solids **60**, 145 (1999).
[259] J. Haines, C. Chateau, J. M. Leger, and R. Marchand, Ann. Chim. Sci. Mater. **26**, 209 (2001).
[260] A. P. Young, Z. Kristallogr. **118**, 223 (1963).
[261] S. M. Clark, A. G. Christy, R. Jones, J. Chen, J. Chen, J. M. Thomas, and G. N. Greaves, Phys. Rev. B **51**, 38 (1995).
[262] J. Badro, P. H. Gillet, P. F. McMillan, A. Polian, and J. P. Itié, Europhys. Lett. **40**, 533 (1997).
[263] J. M. Gallardo-Amores, U. Amador, E. Morán, and A. Vegas, High Press. Res. **22**, 577 (2002).
[264] D. Santamaría-Pérez, J. Haines, U. Amador, E. Morán, and A. Vegas, Acta Crystallogr. B **62**, 1019 (2006).
[265] J. L. Robeson, R. R. Winters, and W. S. Hammack, Phys. Rev. Lett. **73**, 1644 (1994).
[266] J. Badro, J. P. Itié, and A. Polian, Eur. Phys. J. B **1**, 265 (1998).
[267] M. B. Krueger and R. Jeanloz, Science **249**, 647 (1990).
[268] J. S. Tse and D. D. Klug, Science **255**, 1559 (1992).
[269] A. Polian, M. Gimsditch, and E. Philippot, Phys. Rev. Lett. **71**, 3143 (1993).
[270] J. Haines, C. Chateau, J. M. Léger, C. Bogicevic, S. Hull, D. D. Klug, and J. S. Tse, Phys. Rev. Lett. **91**, 015503 (2003).
[271] M. P. Pasternak, G. Kh. Rozenberg, A. P. Milner, M. Amanowicz, T. Zhou, U. Schwarz, K. Syassen, R. D. Taylor, M. Hanfland, and K. Brister, Phys. Rev. Lett. **79**, 4409 (1997).
[272] J. Pellicer-Porres, A. M. Saitta, A. Polian, J. P. Itié, and M. Hanfland, Nature Mater. **6**, 698 (2007).
[273] T. Yagi, Nature Mater. **5**, 935 (2006).
[274] L. Huang, M. Durandurdu, and J. Kieffer, Nature Mater. **5**, 977 (2006).
[275] A. E. Ringwood and A. Major, Earth Planet. Sci. Lett. **1**, 241 (1966).
[276] S. Akimoto and H. Fujisawa, J. Geophys. Res. **73**, 1467 (1968).
[277] N. Morimoto, S. Akimoto, K. Koto, and M. Tokonami, Science **165**, 586 (1969).
[278] L. G. Liu, Nature **262**, 770 (1976).
[279] H. Morishima, T. Kato, M. Suto, E. Ohtani, S. Urakawa, W. Utsumi, O. Shimomura, and T. Kikegawa, Science **265**, 1202 (1994).
[280] T. Irifune, N. Nishiyama, K. Kuroda, T. Inoue, M. Isshiki, W. Utsumi, K. Funakoshi, S. Urakawa, T. Uchida, T. Katsura, and O. Ohtaka, Science **279**, 1698 (1998).
[281] T. Irifune, Y. Higo, T. Inoue, Y. Kono, H. Ohfuji, and K. Funakoshi, Nature **451**, 814 (2008).
[282] S. V. Ovsyannikov, V. V. Shchennikov, S. Todo, and Y. Uwatoko, J. Phys.: Condens. Matter **20**, 172201 (2008).
[283] A. E. Ringwood and A. F. Reid, Earth Planet. Sci. Lett. **5**, 245 (1969).
[284] Y. W. Fei, D. J. Frost, H. K. Mao, C. T. Prewitt, and D. Häusermann, Am. Mineral. **84**, 203 (1999).
[285] C. Haavik, S. Stolen, H. Fjellvag, M. Hanfland, and D. Häusermann, Am. Mineral. **85**, 514 (2000).
[286] L. S. Dubrovinsky, N. A. Dubrovinskaia, C. McCammon, G. K. Rozenberg, R. Ahuja, J. M. Osorio-Guillen, V. Dmitriev, H. P. Weber, T. Le Bihan, and B. Johansson, J. Phys.: Condens. Matter **15**, 7697 (2003).
[287] P. Lazor, O. N. Shebanova, and H. Annersten, J. Geophys. Res. **109**, B05201 (2004).
[288] Y. Moritomo, Y. Ohishi, A. Kuriki, E. Nishibori, M. Takata, and M. Sakata, J. Phys. Soc. Jpn. **72**, 765 (2003).

[289] H. J. Reichmann and S. D. Jacobsen, Am. Mineral. **91**, 1049 (2006).
[290] A. M. Pendás, A. Costales, M. A. Blanco, J. M. Recio, and V. Luaña, Phys. Rev. B **62**, 13970 (2000).
[291] J. M. Recio, R. Franco, A. M. Pendás, M. A. Blanco, L. Pueyo, and R. Pandey, Phys. Rev. B **63**, 184101 (2001).
[292] L. Gerward, A. Waskowska, J. Staun Olsen, J. M. Recio, and M. Marqués, to be published in High Press. Res.
[293] T. Irifune, K. Fujino, and E. Ohtani, Proc. US-Japan Conf., Ise, Japan, 1991.
[294] A. Chopelas and A. M. Hofmeister, Phys. Chem. Miner. **18**, 279 (1991).
[295] M. Catti, F. F. Fava, C. Zicovich, and R. Dovesi, Phys. Chem. Miner. **26**, 389 (1999).
[296] D. Levy, A. Pavese, A. Sani, and V. Pischedda, Phys. Chem. Miner. **28**, 612 (2001).
[297] Z. W. Wang, R. T. Downs, V. Pischedda, R. Shetty, S. K. Saxena, C. S. Zha, Y. S. Zhao, D. Schiferl, and A. Waskowska, Phys. Rev. B **68**, 094101 (2003).
[298] L. Malavasi, C. Tealdi, G. Flor, and M. Amboage, Phys. Rev. B **71**, 174102 (2005).
[299] A. Waskowska, L. Gerward, J. Staun Olsen, M. Feliz, R. Llusar, L. Gracia, M. Marqués, and J. M. Recio, J. Phys.: Condens. Matter **16**, 53 (2004).
[300] V. V. Ursaki, F. J. Manjón, I. M. Tiginyanu, and V. E. Tezlevan, J. Phys.: Condens. Matter **14**, 6801 (2002).
[301] F. J. Manjón, A. Segura, M. Amboage, J. Pellicer-Porres, J. F. Sánchez-Royo, J. P. Itié, A. M. Flank, P. Lagarde, A. Polian, V.V. Ursaki, and I. M. Tiginyanu, Phys. Status Solidi B **244**, 229 (2007).
[302] J. Ruiz-Fuertes, D. Errandonea, F. J. Manjón, D. Martínez-García, A. Segura, V. V. Ursaki, and I. M. Tiginyanu, J. Appl. Phys. **103**, 063710 (2008).
[303] A. Zerr, G. Miehe, G. Serghiou, M. Schwarz, E. Kroke, R. Riedel, H. Fuess, P. Kroll, and R. Boehler, Nature **400**, 340 (1999).
[304] H. L. He, T. Sekine, T. Kobayashi, H. Hirosaki, and I. Suzuki, Phys. Rev. B **62**, 11412 (2000).
[305] P. F. McMillan, O. Shebanova, D. Daisenberger, R. Quesada, E. Bailey, A. Hector, V. Lees, D. Machon, A. Sella, and M. Wilson, Phase Transit. **80**, 1003 (2007).
[306] A. Grzechnik, V. V. Ursaki, K. Syassen, I. Loa, I. M. Tiginyanu, and M. Hanfland, J. Solid State Chem. **160**, 205 (2001).
[307] S. Meenakshi, V. Vijyakumar, B. K. Godwal, A. Eifler, I. Orgzall, S. Tkachev, and H. D. Hochheimer, J. Phys. Chem. Solids **67**, 1660 (2006).
[308] D. Errandonea, R. S. Kumar, F. J. Manjón, V. V. Ursaki, and I. M. Tiginyanu, J. Appl. Phys. **104**, 063524 (2008).
[309] M. O'Keeffe and B. G. Hyde, The role of non-bonded forces in crystals, in: Structure and Bonding in Crystals, Vol. 1 (Academic Press, New York, 1981), p. 227.
[310] M. O'Keeffe, Some Aspects of the Ionic Model of Crystals, in: Structure and Bonding in Crystals, Vol. 1 (Academic Press, New York, 1981), p. 299.